

PNEUMATIC SWITCHING OF THE OPTICAL POWER OF A FRESNEL LENS FOR
CONTROL OF SOLAR ILLUMINATION

by

ERI WATANABE

B.Sc, Dalhousie University, 2007

A THESIS SUBMITTED IN PARTIAL FULFILLMENT OF
THE REQUIREMENTS FOR THE DEGREE OF
MASTER OF SCIENCE

in

THE FACULTY OF GRADUATE STUDIES

(Physics)

THE UNIVERSITY OF BRITISH COLUMBIA
(VANCOUVER)

AUGUST, 2009

© Eri Watanabe, 2009

ABSTRACT

A pneumatic-based illumination switch has been developed for use in conjunction with collimated daylighting collection systems that collect sunlight on the façade of a multi-storey building and distribute it throughout the core areas of the building. Daylight collection systems are currently of interest since they have the potential to significantly reduce the need for electrical lighting in workplaces, thus reducing the required electrical energy and associated greenhouse gas emissions. In one particular system, sunlight is distributed by hollow light guides and redirected into light fixtures positioned along the guides. The illumination switch described here can be incorporated into the light guides to control the amount of sunlight that is directed into each fixture. This control device consisted of a Fresnel lens positioned with its structured surface adjacent to a layer of silicone gel that had a similar refractive index value as the lens. In one mode of operation, the gel layer was separated from the lens so that the lens focused incident sunlight into a hollow light guide that carried the sunlight to a fixture. In the second mode of operation, when the index-matching gel layer was pressed into contact with the structured surface of the Fresnel lens, the switch allowed sunlight to pass substantially undeflected through the lens and continued down the guide. The switch was activated by a vacuum pump that adjusted the relative pressure in order to pull the silicone gel into and out of contact with the Fresnel lens. Experimental tests showed that intensity of the light emitted by a fixture can be controllably and reproducibly reduced by about 75 % of the original intensity when the switch was activated.

TABLE OF CONTENTS

ABSTRACT	ii
TABLE OF CONTENTS	iii
LIST OF TABLES	vi
LIST OF FIGURES	vii
ACKNOWLEDGEMENTS	ix
1 INTRODUCTION	1
2 BACKGROUND	5
2.1 COLLIMATED DAYLIGHTING SYSTEM	5
2.1.1 Solar Canopy Illumination System.....	5
2.1.1.1 Collection of sunlight.....	6
2.1.1.2 Distribution of sunlight.....	7
2.2 INDEX OF REFRACTION	8
2.3 TOTAL INTERNAL REFLECTION.....	9
3 DESIGN OF THE ILLUMINATION SWITCH	10
3.1 BASIC PRINCIPLE OF THE DESIGN OF THE ILLUMINATION SWITCH.....	10
3.2 METHOD OF DEFORMING THE SILICONE GEL.....	12
3.3 LIGHT GUIDING DEVICES	12
3.3.1 Optical Fiber	13
3.3.2 Enhanced Specular Reflector Films.....	14
3.4 FRESNEL LENSES	14
3.4.1 Choosing a Fresnel Lens.....	16
3.5 SILICONE GEL.....	19
3.5.1 Choosing a Silicone Gel	20
3.5.2 Hysteresis of the Silicone Gel.....	20
3.5.3 UV Treatment on the Silicone Gel	21

4	CONSTRUCTION OF THE ILLUMINATION SWITCH	23
4.1	CONSTRUCTION OF THE ILLUMINATION SWITCH	23
4.1.1	Detailed Design of the Illumination Switch	23
4.1.2	Air Channel on the Fresnel Lens	25
4.1.3	Deformation of the Silicone Gel.....	26
4.2	PNEUMATIC COMPONENT OF THE ILLUMINATION SWITCH	27
5	EXPERIMENTAL RESULTS.....	30
5.1	METHODS OF MEASUREMENT.....	30
5.1.1	Integrating Detector	30
5.1.2	Producing a Collimated Beam	32
5.1.3	Measuring the Pressure.....	34
5.2	HYSTERESIS OF THE SILICONE GEL	34
5.3	INTENSITY CHANGE WITH AMOUNT OF UV TREATMENT.....	35
5.4	MEASURING THE RELATIVE ADHESIVENESS OF THE SILICONE GEL WITH DIFFERENT UV TREATMENT TIME	37
5.5	UV TREATMENT ON THE SURFACE OF THE SILICONE GEL	40
5.6	ENDURANCE OF THE ILLUMINATION SWITCH.....	42
5.6.1	Endurance of the Device After Many Switch Cycles	42
5.6.2	Endurance Under Different Temperature Conditions.....	45
5.6.2.1	Lower temperature test	45
5.6.2.2	Higher temperature test.....	48
6	RAY TRACE MODELING	50
6.1	MODELING WITH A MONTE CARLO RAY TRACING SOFTWARE.....	50
6.1.1	Model Set-Up on Monte Carlo Ray Tracing Program.....	50
6.1.2	Model Results on Change in Intensity.....	54
6.2	COMPARISON WITH THE EXPERIMENTAL RESULT	55
6.3	MODELING THE ESR FILM TUBES AND OPTICAL FIBERS	56
6.3.1	Comparison of ESR Film Tube and Optical Fiber on TracePro.....	56
6.3.2	Advantages and Disadvantages of the ESR Film Tube and Optical Fiber	60
7	DEMONSTRATION OF THE ILLUMINATION SWITCH IN A LIGHT GUIDANCE SYSTEM.....	61
7.1	SET UP OF THE DEMONSTRATION.....	61
7.2	CONSTRUCTED DEMONSTRATION SYSTEM.....	63

8 CONCLUSION	65
REFERENCES.....	68
APPENDIX A: UV LAMP	73
APPENDIX B: SILICONE GEL.....	74
APPENDIX C: FRESNEL LENS.....	75
APPENDIX D: RAY TRACE MODELING	76
APPENDIX E: PICTURES OF THE DEMONSTRATION SET UP.....	78

LIST OF TABLES

TABLE 3-1. TABLE OF SPECIFICATIONS OF THE TWO FRESNEL LENSES	19
TABLE 6-1. EMISSIVITY IMPUTED FOR SIMULATING THE LIGHT SOURCE ON TRACEPRO	53
TABLE 6-2. TRANSMITTANCE LOSS FOR THE BEST-CASE SCENARIO	58
TABLE 6-3. TRANSMITTANCE LOSS FOR THE WORST-CASE SCENARIO	59
TABLE 7-1. ILLUMINATION LEVEL OF THE LIGHT BULBS.....	63
TABLE B- 1. PROPERTIES OF THE SILICONE GEL FROM DOW CORNING ⁷⁹	74
TABLE C- 1. PROPERTIES OF THE FRESNEL LENS FROM EDMUND OPTICS ⁸⁰	75

LIST OF FIGURES

FIGURE 2-1. DIAGRAM OF THE SOLAR CANOPY ILLUMINATION SYSTEM (NOT TO SCALE).....	6
FIGURE 2-2. DIAGRAM OF ARRAY OF MIRRORS CONTROLLED BY AN ACTUATOR TO TRACK THE SUN... 7	7
FIGURE 2-3. SIDE VIEW OF THE DUAL-FUNCTION LIGHT GUIDE	8
FIGURE 3-1. CONFIGURATION OF THE DEVICE WHEN THE FRESNEL LENS IS ACTIVE	11
FIGURE 3-2. CONFIGURATION OF THE DEVICE WHEN THE FRESNEL LENS IS DEACTIVATED	11
FIGURE 3-3. INCREASING THE PRESSURE VERSUS DECREASING IT	12
FIGURE 3-4. ACCEPTANCE ANGLE OF AN OPTICAL FIBER.....	13
FIGURE 3-5. COMPARISON OF A PLANO-CONVEX LENS AND A FRESNEL LENS.....	15
FIGURE 3-6. SCHEMATIC DIAGRAM OF (A) A CONVERGING AND (B) A DIVERGING FRESNEL LENS.....	15
FIGURE 3-7. WAIST OF A FRESNEL LENS	17
FIGURE 3-8. HEIGHT OF THE PRISM AND GROOVES (NOT TO SCALE).....	18
FIGURE 3-9. DIAGRAM OF THE HARD LAYER CREATED BY UV TREATMENT ON THE GEL (NOT TO SCALE).....	22
FIGURE 4-1. SCHEMATIC DIAGRAM OF THE CROSS-SECTION OF THE ILLUMINATION SWITCH.....	23
FIGURE 4-2. SCHEMATIC DIAGRAMS OF (A) THE ALUMINUM FRAME, (B) THE ACRYLIC COVER, AND (C) THE FRESNEL LENS (NOT TO SCALE)	24
FIGURE 4-3. A SCHEMATIC DIAGRAM OF THE FRESNEL LENS SHOWING (A) THE AREA WHERE THE AIR WAS PUMPED OUT (SHADED REGION) AND THE AREA WHERE THE AIR WAS TRAPPED (NOT SHADED REGION) AND (B) AN AIR CHANNEL	25
FIGURE 4-4. A CLOSER LOOK AT THE AIR CHANNEL ON THE FRESNEL LENS (SIDE VIEW, NOT TO SCALE).....	26
FIGURE 4-5. (A) PERFECTLY DEFORMED SILICONE GEL ON TRACEPRO AND (B) ACTUAL DEFORMED SILICONE GEL WHICH IS NOT PERFECTLY DEFORMED	26
FIGURE 4-6. DIAGRAM OF THE 3/2 WAY VALVE SHOWING THE AIR FLOW	27
FIGURE 4-7. DIAGRAM OF THE 2/2 WAY VALVE SHOWING THE AIR FLOW	28
FIGURE 4-8. SCHEMATIC DIAGRAM OF THE PNEUMATIC PART OF THE ILLUMINATION SWITCH.....	29
FIGURE 5-1. SCHEMATIC DIAGRAM OF THE INTEGRATING DETECTOR	30
FIGURE 5-2. SCHEMATIC DIAGRAM OF THE OPTICAL PART OF THE MEASUREMENT SYSTEM.....	31
FIGURE 5-3. DIAGRAM SHOWING THE ANGLE θ	33
FIGURE 5-4. INTENSITY DISTRIBUTION OF LIGHT SOURCE.....	33
FIGURE 5-5. HYSTERESIS OF THE SILICONE GEL IN THE ILLUMINATION SWITCH	35
FIGURE 5-6. CHANGE IN INTENSITY USING SILICONE GELS WITH DIFFERENT DURATION OF UV TREATMENT WITH F=7.5 CM FRESNEL LENS	37
FIGURE 5-7. SET UP OF THE RELATIVE ADHESION TEST.....	38
FIGURE 5-8. ACCELERATION OF THE BALL.....	39
FIGURE 5-9. GRAPHS OF X AND Y POSITIONS OF THE BALL AS A FUNCTION OF TIME	39
FIGURE 5-10. ADHESION OF THE SILICONE GEL WITH VARIOUS UV TREATMENT TIMES	40
FIGURE 5-11. (A) DIAGRAM OF THE SAMPLE SILICONE GEL AND (B) ESEM IMAGES OF THE GEL WITHOUT UV TREATMENT AND AFTER FOUR HOURS OF UV TREATMENT.....	42
FIGURE 5-12. A TYPICAL EXAMPLE OF ONE SWITCH CYCLE.....	43
FIGURE 5-13. ENDURANCE TEST DUE TO THE NUMBER OF SWITCH CYCLES	44
FIGURE 5-14. TIME FOR THE GEL TO SEPARATE FROM THE LENS	45
FIGURE 5-15. SET UP FOR LOWER TEMPERATURE TEST	46
FIGURE 5-16. CHANGE IN INTENSITY OF THE ILLUMINATION SWITCH AND TEMPERATURE WITHIN THE ACRYLIC BOX WITH RESPECT TO TIME	47
FIGURE 5-17. RELATIVE INTENSITY VS. PRESSURE GRAPH FOR LOWER TEMPERATURE TEST	48
FIGURE 5-18. SET UP OF THE HIGHER TEMPERATURE TEST	48

FIGURE 5-19. TEMPERATURE AND CHANGE IN INTENSITY AS A FUNCTION OF TIME FOR HIGHER TEMPERATURE EXPERIMENT	49
FIGURE 6-1. SET UP FOR THE RAY TRACING MODELING (A) WHEN FRESNEL LENS IS DEACTIVATED AND (B) ACTIVATED (NOT TO SCALE).....	51
FIGURE 6-2. SCHEMATIC DIAGRAM OF THE (A) GEOMETRY OF SIMULATED FRESNEL LENS ON TRACEPRO AND (B) THE ACTUAL FRESNEL LENS FOR THE ILLUMINATION SWITCH	52
FIGURE 6-3. GRAPHS OF EXPERIMENTALLY MEASURED INTENSITY LEVEL OF THE MR16 AND THAT OF SIMULATED LIGHT SOURCE	53
FIGURE 6-4. SIMULATED RAYS ON TRACEPRO (RAYS THAT DOES NOT GO THROUGH THE FOCAL POINT ARE THE MISBEHAVED RAYS).....	54
FIGURE 6-5. IMAGES FROM TRACEPRO WHEN THE DEVICE IS (A) DEACTIVATED AND (B) ACTIVATED	55
FIGURE 6-6. SET UP OF THE RAY TRACING FOR COMPARING THE OPTICAL FIBER AND ESR FILM TUBE	57
FIGURE 7-1. SCHEMATIC DIAGRAM OF THE DEMONSTRATION WHEN THE LENS WAS (A) ACTIVATED AND (B) DEACTIVATED.....	62
FIGURE 7-2. PHOTOGRAPHS OF THE LIGHT BULBS WHEN THE LENS WAS ACTIVATED AND DEACTIVATED (THE LIGHT BULBS ARE USED ONLY FOR DIFFUSING PURPOSE).....	64
FIGURE A- 1. SPECTRAL DISTRIBUTION OF THE MERCURY BULB USED FOR THE UV LAMP ⁷⁷	73
FIGURE C- 1. SPECTRAL TRANSMISSION OF THE FRESNEL LENS ⁸¹	75
FIGURE D- 1. SIMULATED SILICONE GEL BY “SUBTRACTION”	76
FIGURE D- 2. AN EXAMPLE OF POLAR ISO-CANDELA PLOT.....	77
FIGURE E- 1. PICTURE OF THE DEMONSTRATION SET UP.....	78
FIGURE E- 2. CLOSER LOOK AT THE SOURCE LIGHT (MR16) AND LIGHT GUIDE	79
FIGURE E- 3. CLOSER LOOK AT THE ILLUMINATION SWITCH AND OTHER OPTICAL COMPONENTS	80

ACKNOWLEDGEMENTS

I would like to express many thanks to the past and present team members of Structured Surface Physics Laboratory. In particular, I would like to thank Peter Friedel, Steven Gou, Weilai Li, Jason Radel, Allen Upward, and Richard Wong for their assistance and their friendship.

Sincere thanks to my supervisor, Dr. Lorne Whitehead, for providing me with an opportunity to work in such a great lab. His ideas and expertise were very helpful; I learned more about industrial approaches to physics in his lab than I ever could have learned in the classroom.

Thanks to Dr. Andrzej Kotlicki for his helpful advice and assistance. He was very generous with his equipment and provided me with a lot of helpful suggestions. I would also like to thank Dr. Michele Mossman for her ideas and advice as well. She was very kind and patient with her explanations.

I am grateful to NSERC, UBC, and the 3M Company for their financial support throughout the course of this project. Without their financial assistance this project would not have been possible.

Finally, I would like to thank my parents for supporting me during the course of my studies in Canada. I always wanted to be like my mother, who always provides great support for family members, and father, who is both a great scientist and businessman. I would also like to thank my little sister, Mika, who is always supportive and considerate.

1 INTRODUCTION

Sunlight is an inexhaustible natural resource that can help to reduce the need for electrical lighting energy. Utilizing a system that provides daylight for illumination purpose to office buildings will reduce significant amount of electricity consumption of the building since large portion of it is a result of illumination by electric lights. For example, about 40 % of the total electricity consumption in a building comes from illumination in the United States¹. The use of such a system will help to reduce greenhouse gas emissions and also provide natural daylight in workplaces which is thought to be higher quality light for occupants². There have been a number of inventions for using daylight for illumination and there are currently two main approaches to introduce daylight into a building for illumination. The first approach uses diffuse daylighting systems to increase the sunlight entering a building. A diffuse daylighting system is capable of introducing diffuse daylight into a building. Light shelves³, skylights⁴ and anidolic daylight systems⁵ fall into this category. One of the most common diffuse daylighting systems is the use of tall windows which can be seen in many current office buildings. Tall windows allow more daylight into the building than conventional windows which tend to be shorter. Another example of diffuse daylighting systems is the light shelves. The light shelves enhance more daylight to enter a building by locating a sheet of reflective material outside or inside of the building near windows. These sheets reflect the incident sunlight to ceilings which makes inner part of the building brighter than using the tall windows alone. Skylights are flat or domed windows which are typically mounted horizontally on roof tops so that daylight can reach inner part of a building. Anidolic daylighting system uses parabolic mirrors to redirect the daylight into light guides for illumination.

Although these diffuse daylighting systems help illumination, they are not very effective in terms of cost and energy savings. For example, tall windows are more expensive than conventional shorter windows and cannot illuminate the building core, since the sunlight only penetrates a short distance into the building. Furthermore, the light tends to enter sideways through the window, rather than downwards from above, and this sideways light causes discomfort glare for the occupants. These tall windows also produce high heat in the

building which adds the cost of cooling the building. To reduce heating from sunlight, low transmission glazing can be installed and there are many studies associated with window glazing^{6,7,8} which are aimed to overcome these issues but the cost of producing such windows is very high. Also, using low transmission glazing may not be acceptable to occupants since more glazing transmits less daylight which makes the room appear dim and fails to function as diffuse daylighting systems⁹. For the case of light shelves, the heat gain can be reduced by the shade created by the reflective sheet on the windows¹⁰ but they cannot provide constant and uniform illumination throughout a day since the intensity level of daylight changes depending on climate and time of the day. This is an issue also for the skylights and anidolic daylight systems.

The second approach for bringing daylight into a building is the use of collimated daylighting systems. A collimated daylighting system can provide daylight to core part of a building for illumination, unlike a diffuse daylighting system which provides daylight to only a small fraction of area, by maintaining a certain degree of collimation of the collected sunlight. These systems typically have a sunlight collection component and a distribution component to collect and bring the sunlight into a core region of a building. The idea of a sunlight collection and guiding system is not new, and a number of collimated daylighting for illumination have been previously developed^{11,12}. SolarPoint Lighting¹³ manufactured by Sunlight Direct is one commercially available collimated daylighting systems. SolarPoint Lighting uses parabolic mirrors to concentrate daylight at optical fibers which carry the collected daylight throughout a building. The parabolic mirrors are controlled so that it tracks the sun accurately. Another example of a commercially available system is Parans Solar Lighting System¹⁴. The daylight collection component of this system consists of many Fresnel lenses which are moved by an active tracking which keeps the surface of the Fresnel lenses perpendicular to the direction of the sunlight¹⁵. This tracking is controlled by photosensors which record the intensity level of daylight throughout the day when this system is initially installed. Then, they store the motion of the sun at the location of the building based on the recorded measured intensity level. The Fresnel lenses are moved by this tracking system and collect sunlight by concentrating the sunlight at optical fibers which are located at the lens' focal length which then carry the collected sunlight throughout the building.

Both systems are able to accurately track the sun so their concentration ratio is very high. However, these systems are not cost effective since the optical components are required to be very precise in order to produce the high concentration ratio. The comparative cost of optical fibers throughout the building is also another reason why these collimated daylighting systems are not cost effective.

One collimated daylighting system recently developed at University of British Columbia¹⁶ appears to have the potential to be cost effective in volume production. The so-called solar canopy illumination system is a sunlight collection and guiding system and is targeted for multi-storey office buildings since collection modules can be installed on each floor, above the windows. This collection system can be used in new construction and also requires minimal renovation in order to be installed in many existing buildings. Using this system, the existing electric lighting system can be replaced with dual function light guides that operate as efficient electric fixtures and also distribute sunlight to the core regions of the building. The sunlight collection system on the exterior has the added benefit of providing shade for the windows, which reduces the need for window filters and also reduces electrical energy required for air conditioning. The first demonstration system based on this technology was successfully completed on an existing building in Vancouver, Canada in 2008¹⁷, and more installations are currently underway. This solar canopy illumination system can be cost effective since the concentration ratio is about 10, which is low compared to the other collimated daylighting systems, so the optical components are not required to be highly precise which reduce the cost of the components but still able to collect and distribute the required amount of sunlight.

Utilizing these collimated daylighting systems, the need for electrical lighting can be reduced significantly since they can bring daylight to core regions of a building to replace electrical lightings. However, since the amount of sunlight that strikes the façade of the building is limited, it is advantageous to use the sunlight only where it is needed. To facilitate this, an illumination switch can be used to adjust the illumination level of different fixtures, so that the sunlight can be redirected to other areas of the building. This thesis describes the design and performance of a pneumatic-based illumination switch that can be used in collimated daylighting systems. The illumination switch controls the light intensity level by varying the

optical power of a Fresnel lens by controllably forcing it into contact with a sheet of transparent silicone gel that has a similar index of refraction value as the Fresnel lens.

The background information of the sunlight collection system and other basic physical principles associated with the sunlight collection system and the pneumatic-based illumination switch are described in Chapter 2. The basic concept of the design of the illumination switch using a Fresnel lens and silicone gel is described in Chapter 3 and the details of the construction of the switch are presented in Chapter 4. In Chapter 5, the performance of the experimental device is discussed. The ray trace model of the device and its results are discussed and compared with experimental results in Chapter 6 and a demonstration of the switch in a simple light guiding arrangement is described in Chapter 7. Lastly, the conclusion of this project is presented in Chapter 8.

2 BACKGROUND

In this chapter, background information associated with the collimated daylighting systems and some physical principles used in this project are described.

2.1 COLLIMATED DAYLIGHTING SYSTEM

Although sunlight is a practical source of illumination, at present in most multi-storey office buildings, adequate illumination can only be achieved in a relatively small area around the perimeter of the buildings, typically by the window light that falls within 3 m of the windows. In contrast, collimated daylighting systems are capable of harvesting sunlight on the exterior of the building and distributing it throughout. There are a number of different sunlight collectors invented previously as explained in the introduction, but one example of a practical collimated daylighting system is the solar canopy illumination system¹⁸. The solar canopy illumination system is to our knowledge the first cost-effective sunlight collection system targeted at multi-storey office buildings. As was mentioned in the introduction, this system not only reduces the need for illumination but it also reduces electrical energy needed for cooling the building for high sun elevations as it provides shade for the windows. Utilizing this system helps reduce greenhouse gases and provides better quality light than electric lighting^{19,20}.

2.1.1 Solar Canopy Illumination System

The solar canopy illumination system consists of two main parts; the sunlight collection system and the guiding system. Figure 2-1 shows the schematic diagram of the solar canopy illumination system. The sunlight collection component, as labeled in Figure 2-1, is located on the external façade. In order to maximize the amount of sunlight that can be collected, it is preferable for this solar canopy illumination system to be mounted on the equatorial-facing wall, which in North America is the south wall. The lower part in the diagram shows the sunlight guiding and distribution system. Detailed explanations of these two parts are discussed in section 2.1.1.1 and 2.1.1.2.

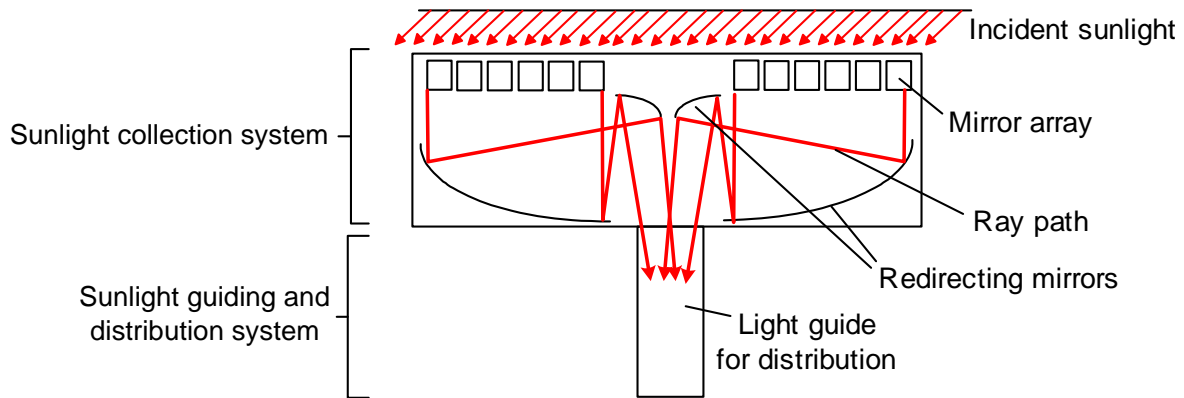


Figure 2-1. Diagram of the solar canopy illumination system (not to scale)

2.1.1.1 Collection of sunlight

As shown in Figure 2-1, each sunlight collection system has two sets of mirror arrays, two small parabolic mirrors, and two large paraboloidal mirrors. This external component of the system collects sunlight using an array of mirrors, referred to as the adaptive butterfly array (Figure 2-2). The motion of the mirrors is controlled by an inexpensive actuator that is programmed so that depending on the geographic location and time of the day and year, the mirrors track the sun accurately in order to maximize the amount of sunlight going into the light guides for illumination. This method of tracking the sun is inexpensive because these mirrors do not have to be very precise and is capable of redirecting sunlight throughout most of the day. The moving mirrors redirect the sunlight toward the large paraboloidal mirror which concentrates the sunlight. The focused sunlight is then recollimated by the small paraboloidal mirror before entering the distribution light guides, through a small entrance window located between the collection and distribution systems. The beam of sunlight entering the building has a resultant collimation angle of about 20° and concentration ratio of about 10 which is estimated to be the value needed for optimal daylighting design²¹. One of the main reasons that previous sunlight collection systems are not cost-effective is that their optical components are required to be very precise since their concentration ratio is very high. The solar canopy illumination system overcame this problem by an optical configuration that is capable of achieving a concentration ratio of 10. The collection modules must be capable of withstanding a wide range of weather conditions since they are

mounted outside of the building. In the case of the solar canopy illumination system, the optical components are enclosed within a transparent canopy which protects them from the elements. This allows relatively inexpensive optical components to use and also eliminates the cost of regular maintenance.

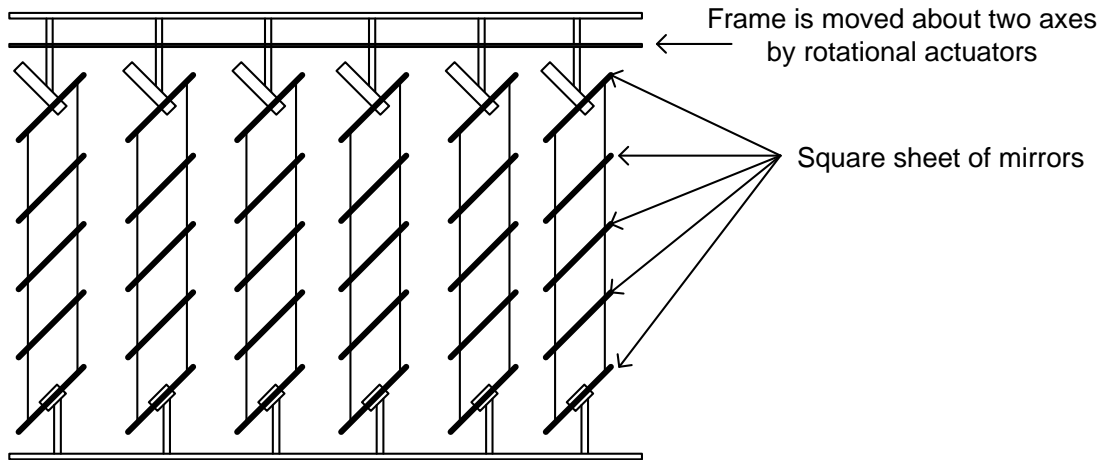


Figure 2-2. Diagram of array of mirrors controlled by an actuator to track the sun

2.1.1.2 Distribution of sunlight

Once the sunlight has been redirected into the building, it is distributed throughout the building by the system referred to as the dual-function prism light guide (Figure 2-3). The light guides can have virtually any cross-sectional shape, but for simplicity a rectangular cross-section has been used in the initial prototypes. The top and side inner surfaces of the guide is covered with a highly reflective multilayer dielectric film²² which has a luminous reflectance value of greater than 98.5 % in the visible wavelength band. The bottom emitting surface of the guide is lined with a sheet of prismatic film which causes total internal reflection when light hits the prismatic film at incident angles greater than a certain critical angle which causes the light to be efficiently transported down the length of the guide, and the high reflectance allows the sunlight to be carried for a long distance with minimal loss. In order to distribute the light for illumination, a sheet of optically diffuse material (typically called an extractor) is used. The extractor is located on the inner top surface of the light guides and it changes the direction of light rays by diffusely reflecting them. As a result, a certain fraction of the light no longer satisfies the conditions for the total internal reflection,

and instead escapes from the light guide by transmitting through the prismatic film. In order to maintain uniform illumination in the building, along the length of the light guide, it is necessary to increase the width of the extractor. This is because as sunlight travels through the building, the amount of sunlight inside of the light guides is reduced and therefore requires a larger sized extractor to distribute greater fraction of sunlight. The amount of sunlight that can be obtained by the collimated daylighting system varies throughout the time of the day and year depending on the hours of sunlight and also the weather conditions. As a result, in order to maintain a constant illumination level, it is necessary to incorporate control system, to supplement the daylight with electric light as necessary.

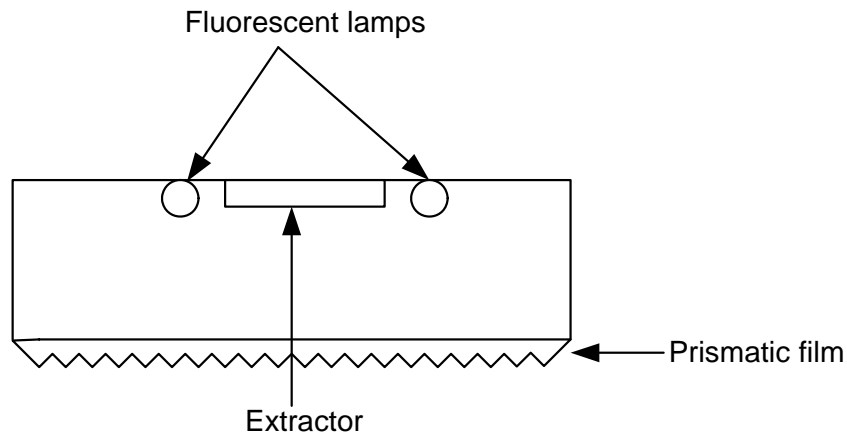


Figure 2-3. Side view of the dual-function light guide

2.2 INDEX OF REFRACTION

A primary design feature for an illumination switch for collimated daylighting systems involves matching the refraction index values of two materials. The concept of index of refraction is also a key to understand the total internal reflection employed by the light guides which will be described in the next section, so for this reason it is important to describe the index of refraction.

The index of refraction of a material is the ratio of the speed of light in vacuum to the speed of light in the material. The value of the refraction index depends on the permittivity and permeability according to the Maxwell equations, where permittivity describes the reduction in total electric field when going through dielectric materials and permeability describes the

degree of magnetization of a material in response to an applied magnetic field. The refraction index is often used for understanding the behavior of a light ray within a material or at the boundary of two materials with different refraction indices.

2.3 TOTAL INTERNAL REFLECTION

As mentioned earlier, the light guides in the solar canopy illumination system employ total internal reflection in order to propagate light throughout the building. It is important to understand the total internal reflection (TIR) as some of the other types of light guiding devices are introduced later on which also employ TIR for transmitting light.

When light travels from one medium to the other, the direction of the outgoing light changes by following the Snell's law of refraction. Snell's law has the form:

$$n_i \sin \theta_i = n_f \sin \theta_f \quad (2.1)$$

where n_i and n_f are the index of refraction of initial medium and the second medium respectively and θ_i is the angle of incidence and θ_f is the angle of the outgoing light ray. When $n_i < n_f$, any angle of incident ray is transmitted into the second medium. On the other hand, some light rays are not transmitted into the second medium when $n_i > n_f$ but reflected at the boundary of the two mediums and stay in the initial medium, and this is the phenomenon known as TIR. This occurs when the incident angle of the light ray is greater than a critical angle, where θ_c is calculated by:

$$\sin \theta_c = \frac{n_f}{n_i} \quad (2.2)$$

The application of the TIR is used for some light guiding devices, such as optical fibers, and these devices are explained more in detail in the next chapter.

3 DESIGN OF THE ILLUMINATION SWITCH

The goal of this project was to design and construct an illumination switch which can be used to vary illumination level of a fixture and also to efficiently distribute sunlight to each fixture by redirecting sunlight to where it is necessary. This can be done by using a Fresnel lens whose optical power can be adjusted in order to control the direction of outgoing light. The optical control is achieved using a layer of soft transparent silicone gel that is index-matched to the Fresnel lens. The detailed design of the device is described in this chapter.

3.1 BASIC PRINCIPLE OF THE DESIGN OF THE ILLUMINATION SWITCH

In this section, the basic principle of the design of the illumination switch is presented. The main parts of the illumination switch consist of a Fresnel lens and a layer of silicone gel where the silicone gel is used in order to change the focusing property of the Fresnel lens.

As Figure 3-1 shows, the transparent silicone gel is positioned adjacent to the Fresnel lens. When the gel is not in contact with the Fresnel lens, the incoming light passes through the silicone gel and is then focused by the Fresnel lens, and a light-guiding device positioned at the focal point of the lens carries the collected sunlight to a specific fixture. In this case, the focusing property of the Fresnel lens is active.

When it is desirable to lower the illumination level of a fixture, the sheet of silicone gel is deformed into the shape of the Fresnel lens. Silicone gel is chosen for deactivating the optical property of the Fresnel lens for its flexibility, high optical transmission and similarity in index of refraction to that of the Fresnel lens. Most Fresnel lenses are made of acrylic which has a typical index of refraction value of 1.5. If the index of refraction of the silicone gel perfectly match that of the Fresnel lens, the prisms of the lens that cause the refraction to focus the light effectively disappear, resulting in no focusing of the incoming light. Rather the light passes through the Fresnel lens undeflected. However, the index of refraction of the silicone gel is typically about 1.4 which is slightly different from the Fresnel lens. Although they are not a perfect match, the divergence of the outgoing light from the lens with

deformed gel is only few degrees. Hence, it was concluded that silicone gel is a practical material to use for this study.

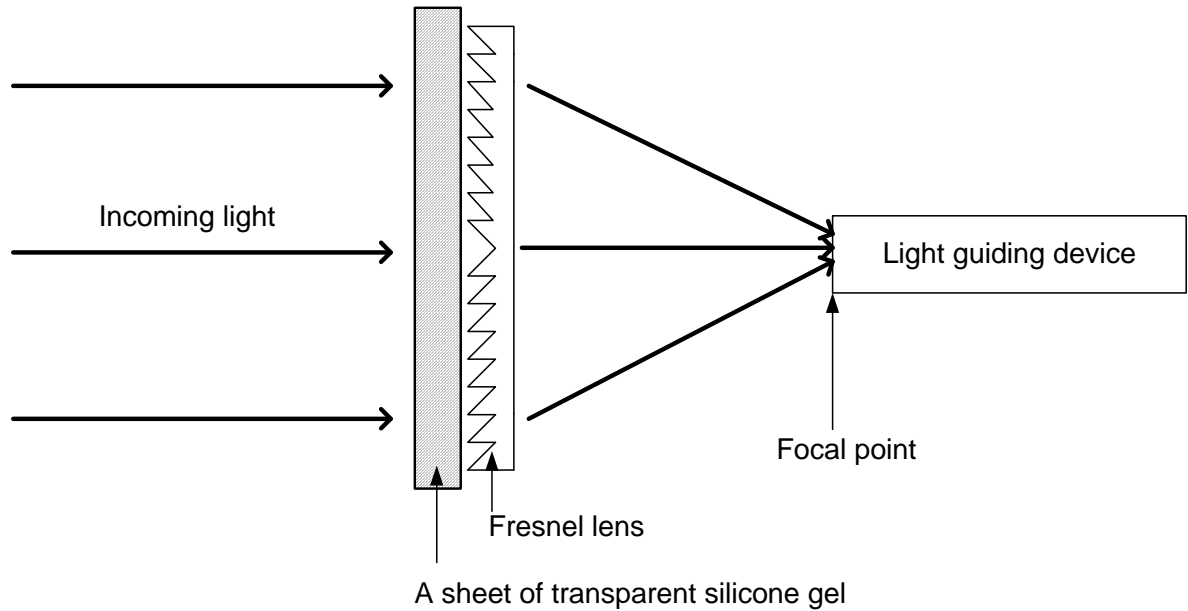


Figure 3-1. Configuration of the device when the Fresnel lens is active

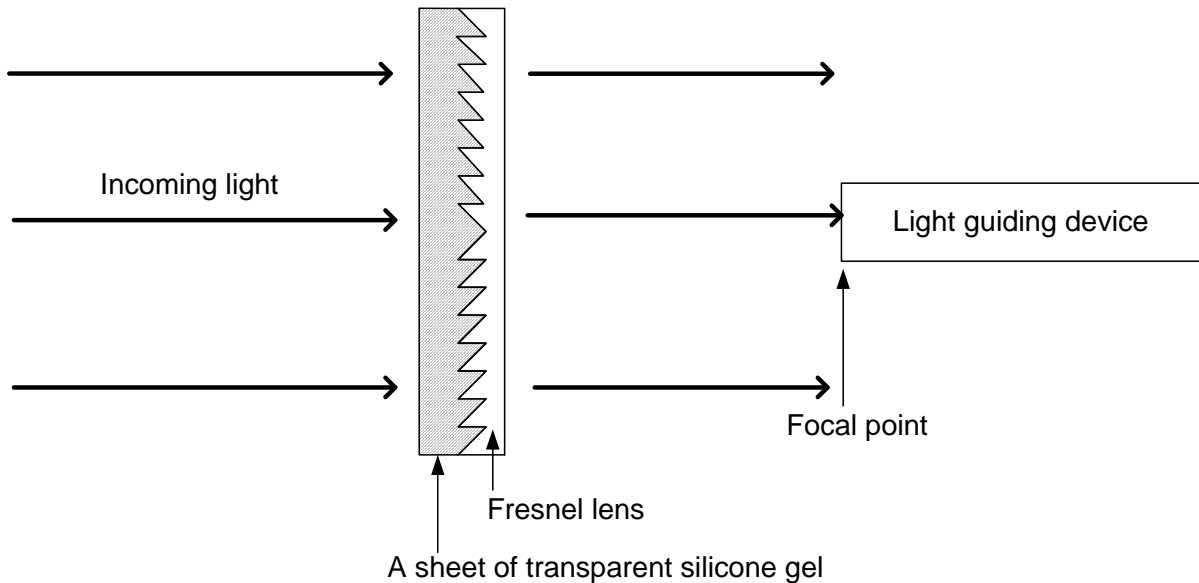


Figure 3-2. Configuration of the device when the Fresnel lens is deactivated

3.2 METHOD OF DEFORMING THE SILICONE GEL

To deform the silicone gel in the shape of the Fresnel lens using a difference in relative pressure, one can either reduce the pressure between the lens and the silicone gel or increase the pressure between the other side of the gel and the device enclosure (Figure 3-3). Since pressurizing the silicone gel from the back can cause explosion if the device fails, a vacuum pump was used to deform the gel for the safety reason.

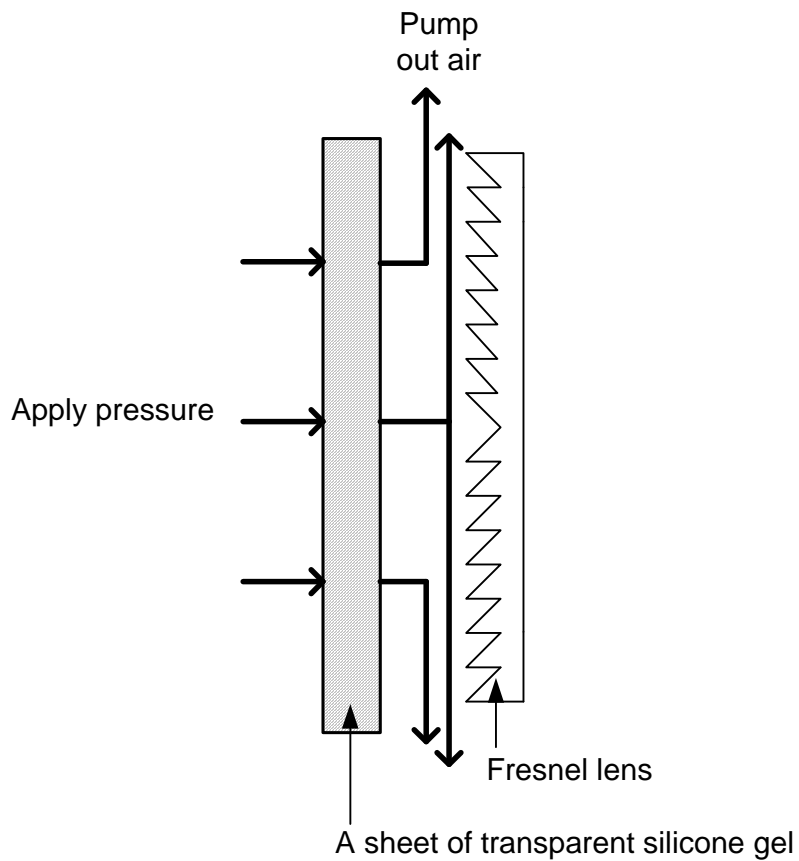


Figure 3-3. Increasing the pressure versus decreasing it

3.3 LIGHT GUIDING DEVICES

In order to select a Fresnel lens for the illumination switch, it was important to consider different light guiding devices since they influenced the choice of the Fresnel lens, which is explained in section 3.4.1. In this section, two different light guiding devices, optical fibers

and Enhanced Specular Reflector (ESR) film tubes, are described since they are the candidates for propagating light in the solar canopy illumination system.

3.3.1 Optical Fiber

A common light transmitting device in recent years is optical fibers which are usually made of plastic or glass, and employ TIR in order to propagate light. They are commonly used in fiber optics communications²³ or as a light guiding devices in some solar energy or lighting applications^{24,25,26}. Index of refraction value of most plastics or glass is about 1.5, so the critical angle is about 40° . Because the incident angle on the front surface of the optical fiber has to be smaller than the critical angle, it limits the angle of the light originally coming into the optical fiber. The angles of incident light which can be guided by the fiber must be less than the so-called acceptance angle²⁷ (Figure 3-4), which for many fiber is about 40° . Incoming light with its divergence of larger than the acceptance angle would not be transmitted which may not be suitable in some cases. It may not be a significant problem for collimated daylighting systems since the sunlight transmitted in the systems has the collimation angle of about 20° as mentioned before which is significantly smaller than the acceptance angle.

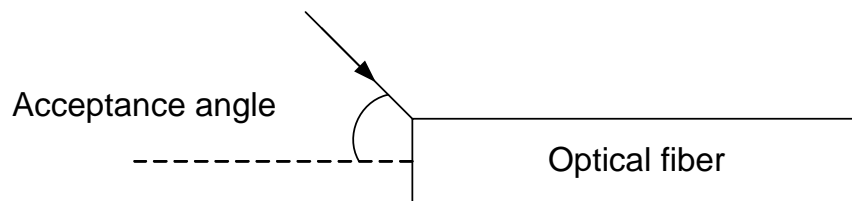


Figure 3-4. Acceptance angle of an optical fiber

When choosing a transmitting device, it is important to consider the attenuation characteristics of the guide, which determine how much of the light intensity is lost for a given distance traveled through the guide. A device with smaller attenuation can transmit light for a longer distance. The attenuation of the optical fiber that was considered to be used for this project had 1.5 % attenuation per foot according to its manufacturer²⁸.

3.3.2 Enhanced Specular Reflector Films

Another option for the light guiding device is to use a hollow tube with a highly reflective inside surface, such as a tube made using Enhanced Specular Reflector (ESR). ESR films are multi-layered optical film that produce high reflectance of light in the visible spectrum and are manufactured by 3M Company²⁹. The reflectance of the film is 98.5 % in the visible spectrum. These tubes are lightweight, preserve the spectral characteristics of the light and may be more efficient than optical fibers in some situations. The attenuation of an ESR film tube occurs when the light hits the surface of the inner film and a small fraction of the light is lost because it is transmitted through the film instead of reflecting and continuing along the tube.

3.4 FRESNEL LENSES

As explained in 3.1, the illumination switch uses Fresnel lens in order to focus the incident light. A Fresnel lens is a thin lens which has the same optical properties as a plano-convex lens³⁰ as shown in Figure 3-5. The main advantage of the Fresnel lens is that it requires less material than a convex lens for its construction. For this reason, the Fresnel lens is lightweight, which is especially advantageous when a large aperture is necessary. Because it is thinner, there is less material for the light to travel through, resulting in less attenuation than a convex lens. The disadvantage is the reduction in image quality due to the fact that the Fresnel lens has discontinuous surfaces. Therefore, the Fresnel lens is not useful to achieve high resolution images but is advantageous for non-imaging applications such as for light concentration purposes.

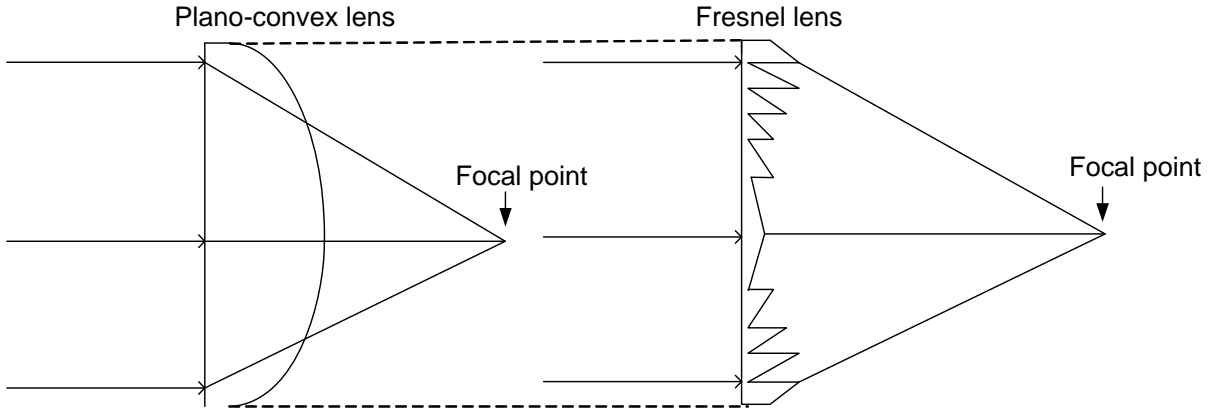


Figure 3-5. Comparison of a plano-convex lens and a Fresnel lens

There are two kinds of Fresnel lenses; converging and diverging Fresnel lenses. As shown in Figure 3-6 (a), a converging Fresnel lens concentrates incoming light at a focal point. A diverging Fresnel lens has an imaginary focal point as shown located on the left side of the lens in Figure 3-6 (b), so the light diverges as it passes through the lens.

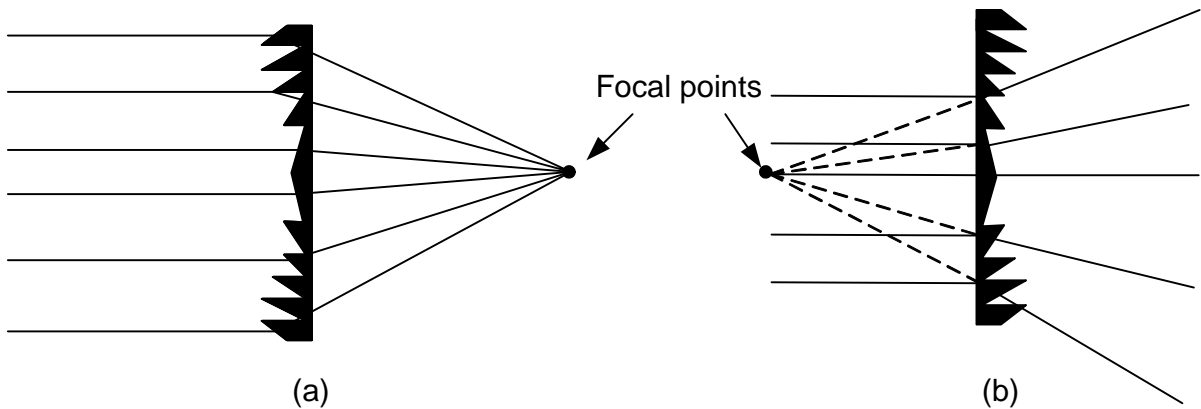


Figure 3-6. Schematic diagram of (a) a converging and (b) a diverging Fresnel lens

Fresnel lenses are used for wide range of applications, such as magnifiers³¹, automotive headlights³², and solar concentrators for photovoltaic devices^{33, 34, 35}. In this project, the converging Fresnel lens was used for the illumination switch in order to focus the incident light at a light guiding device.

3.4.1 Choosing a Fresnel Lens

There were several factors that influenced the choice of the Fresnel lens for the illumination switch. One factor was the focal length of a Fresnel lens since the focal length influences the size of the waist of the lens at the focal point, which is the diameter at the position where the beam is the narrowest³⁶ (Figure 3-7). The size of the opening of a transmitting device should be the same as the waist size so a lens with smaller waist needs a device with smaller opening. For the ideal lens, the waist size is 0 but since the incident light is not always normal to the surface of the lens, it creates a waist bigger than 0. Generally, a lens with a shorter focal length has a smaller waist diameter, than a lens with a longer focal length³⁷. In choosing a Fresnel lens for the illumination switch, the preferred focal length depends on the choice of the light transmitting device. For example, if an ESR film tube is used, it is more preferable to use a lens with a shorter focal length since the waist is smaller, so the diameter of the ESR film tube can be smaller which result in requiring less material to use for light guides. The size of the opening of the transmitting device is preferred to be smaller since it allows smaller amount of light rays entering the device when the Fresnel lens is deactivated. A Fresnel lens with a shorter focal length has smaller waist as mentioned before, which means the opening of the transmitting device can be smaller resulting in obtaining less light entering the transmitting device when the illumination level is desired to be lowered. The ESR film tube does not have an acceptance angle, so there is no need to be concerned about the angle of the incoming light.

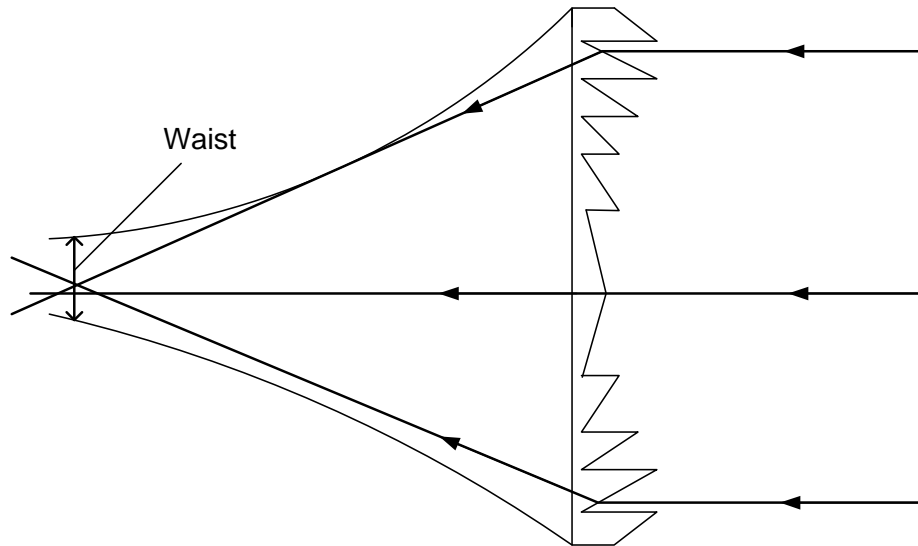


Figure 3-7. Waist of a Fresnel lens

On the other hand, if optical fibers are used as a transmitting device, a lens with a shorter focal length, and therefore a larger divergence angle at the focal point, is not necessarily suitable since optical fibers have a limited acceptance angle. A lens with a shorter focal length causes the light to be more highly divergent, and as a result, the more divergent light rays may not be transmitted by the optical fiber. However, this Fresnel lens with a longer focal length may not be practical since longer focal length lenses have larger waists, and therefore it may not be possible to achieve a sufficient degree of concentration. For this size of the lens, the suitable focal length was estimated to be between 5 cm and 10 cm. A lens with shorter than 5 cm focal length produces light with larger than 35° divergence at the focal point which means some light may not be transmitted if using optical fibers. A lens with its focal length longer than 10 cm was too long because it gave waist of about 4 cm at the focal point. This means that the opening of the light guiding device has to be 4 cm in diameter which means that the area of the opening is close to 50 % of the area of the Fresnel lens. This is too large of an area for the illumination switch to lower the intensity level since a lot of light will enter the light guiding device, even when it is unfocused. As a result of these factors, it was appropriate to choose a lens with an intermediate focal length. For this preliminary study, a readily-available lens with a focal length of 7.5 cm was used. The size of the lens could have been bigger or smaller but it was a good size to start with for the preliminary experiment.

The second factor that influenced the choice of Fresnel lens was the height of the prisms of the Fresnel lens, where the prism height is defined in Figure 3-8. The prism height of the Fresnel lens used in this illumination switch was about 0.1 mm and it was experimentally determined that it required about -50 kPa to obtain the lowest illumination level possible. On the other hand, a Fresnel lens with a prism height of about 0.4 mm manufactured by RHK Japan³⁸ required much more than -70 kPa to obtain the lowest illumination level. It seems reasonable that less pressure is required to force the gel into the lens of the prisms are shorter.

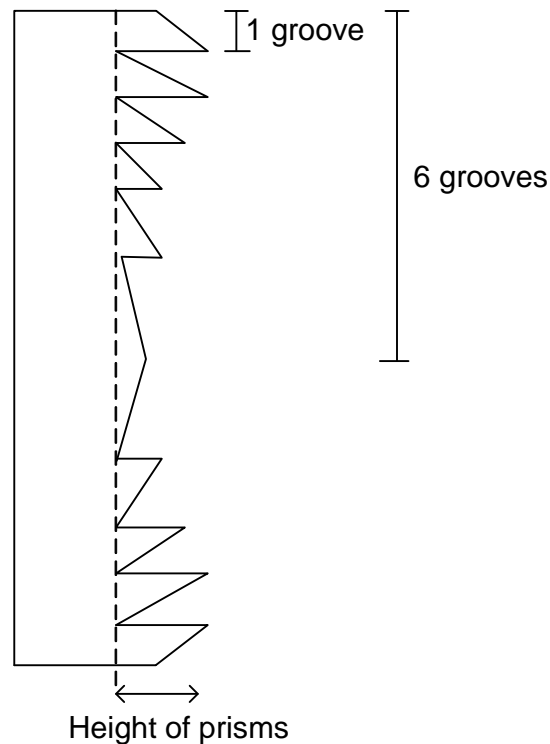


Figure 3-8. Height of the prism and grooves (not to scale)

The number of grooves also affected the choice of the Fresnel lens (see Figure 3-8 for the definition of “a groove”). Two different Fresnel lenses manufactured by Edmund Optics with similar prism height and different number of grooves were compared and their specifications are shown in Table 3-1.

Table 3-1. Table of specifications of the two Fresnel lenses

	Focal length	Height of prism	Number of grooves
Fresnel lens A	20 cm	0.15 cm	25 grooves/ inch
Fresnel lens B	6 cm	0.1 cm	125 grooves/ inch

Although Fresnel lens A³⁹ has slightly higher prisms, it required only about -20 kPa to reach its lowest illumination level. Fresnel lens B⁴⁰, on the other hand, had slightly shorter prism height but it required about -50 kPa to reach the lowest illumination level. It was suspected that the tip of each prism prevented the silicone gel from deforming which led to higher pressure requirement for more number of grooves.

Considering all the factors described above, the Fresnel lens B with a focal length of 7.5 cm was chosen for the illumination switch because the change in intensity of light at the focal point (where the transmitting device was located to transmit light to each fixture) from activated state of the Fresnel lens to deactivated state was maximum meaning that it could lower the illumination level of a fixture more than using other Fresnel lenses.

3.5 SILICONE GEL

Another key component of the illumination switch was the layer of silicone gel. Silicone is widely used as it has desirable properties in a variety of fields. There are a few main reasons for its wide usage. One is the low toxicity of silicones, allowing frequent human contact, such as in medical use⁴¹. Another advantage of using silicone for medical use is its high permeability to gas, such as oxygen⁴². Silicone also has high thermal stability (typical operating range is -40 to 150 °C⁴³) and electrical insulation⁴⁴. Because of these material properties, silicone can be used in extreme conditions. This is why there are adhesives and sealants made with silicones for use inside and outside of buildings. Its flexibility in its shape is also advantageous. It is very easy to create silicones with different shapes since all needed is something to cast it. Some silicones can be cured by room temperature but the typical way of curing silicones is UV light or heat cure. The most common silicone is called

Polydimethylsiloxane (PDMS) and it is made of methyl chloride and silicon. PDMS can be in different forms such as fluid, gel, and elastomers⁴⁵.

In this project, the silicone gel was used for its ability to conform to a neighboring surface and its relatively close match with the refraction index of the acrylic used for the Fresnel lens.

3.5.1 Choosing a Silicone Gel

The important characteristic to consider for choosing gel was its durometer or penetration. Both durometer and penetration is a measure of the hardness of a material, commonly used for elastomers and rubbers, and they are used interchangeably. Durometer is scaled out of 100 and softer materials have a smaller durometer rating. Penetration is measured by applying a fixed force on a ball in contact with the surface of the material and measuring how far it goes into the material. For a penetration measurement, softer materials have higher penetration. The silicone gel used in this project was commercially available Sylgard 524 from Dow Corning⁴⁶ which had a penetration of 4.5 mm. Dow Corning produces a standard clear dielectric silicone gel with penetration of up to 6.0 mm⁴⁷ so the silicone gel with maximum penetration can be used if necessary for the illumination switch.

The Sylgard 524 came in two parts in liquid form and they were cured by mixing them with a 1:1.5 ratio. The refractive index value of this particular silicone gel was 1.41⁴⁸ which was within a typical range for silicone gels. After the two parts were well mixed, it was outgassed in a vacuum chamber to get rid of small air bubbles within the liquid silicone gel. This process was necessary since in the presence of tiny air bubbles, the silicone gel would have slightly different optical properties and this would affect the performance of the illumination switch.

3.5.2 Hysteresis of the Silicone Gel

One interesting characteristic of the silicone gel is that a softer gel tends to be stickier on its surface compared to a harder gel because softer silicone gel contains more oil and water molecules. Since the silicone gel chosen for the illumination switch had to be relatively soft,

it also had a very sticky surface and it produced a so-called hysteresis, which occurs when the response of a physical system depends not only on the magnitude of the input signal applied stress but also on the history of the input signal. In the case of the silicone gel, once the gel was deformed into the lens by applying a pressure on it, it did not separate from the lens even after the pressure was released. Not only did the gel not release itself from the lens, but it also required reversed pressure in order to separate from the Fresnel lens. This phenomenon can be seen in many physical systems and the silicone gel's stickiness on its surface caused an elastic hysteresis which led to a problem described in the next section.

3.5.3 UV Treatment on the Silicone Gel

The sticky surface of the silicone gel prevented it from separating from the Fresnel lens once it was in contact with the lens. For this reason, the surface of the silicone gel needed to be made less sticky, while maintaining the deformation property of the gel. Therefore, using hard silicone gel was not a suitable solution to this problem. This was solved by a UV treatment of the surface of the silicone gel. Illuminating the surface of the silicone gel with UV light is known to create a hard layer on the surface as shown in Figure 3-9, but the exact details of this surface treatment are not well understood. The surface hardening by UV light was done previously for a sheet of PDMS gel in order to produce less adhesion on its surface in order to separate from a structured surface⁴⁹ which is a very similar application to the silicone gel and the Fresnel lens for the illumination switch. It is suspected that shorter wavelength UV light, such as UVC (shorter than 300 nm), causes this surface hardening^{50,51} but not UVA or UVB which has relatively longer wavelengths. The thickness of the hard layer created by the UV treatment varies depending on the amount of UV treatment. Since the height of the prisms used for this project was in order of 0.1 mm, if the hard layer is close to or more than 0.1 mm, then the silicone gel will not be able to deform well into the lens. Therefore, the desirable thickness for the silicone gel in the illumination switch was estimated to be in order of 0.01 mm which was about 1/10 of the height of the prisms. Using the right amount of UV treatment created a very thin hard layer and left the rest of the silicone gel soft enough for deformation. The term "UV treatment" is not the same as "UV cure" in the sense that UV treatment is done after the silicone gel is cured. The particular

silicone gel used in the project cured under room temperature or by heat cure and not with UV light.

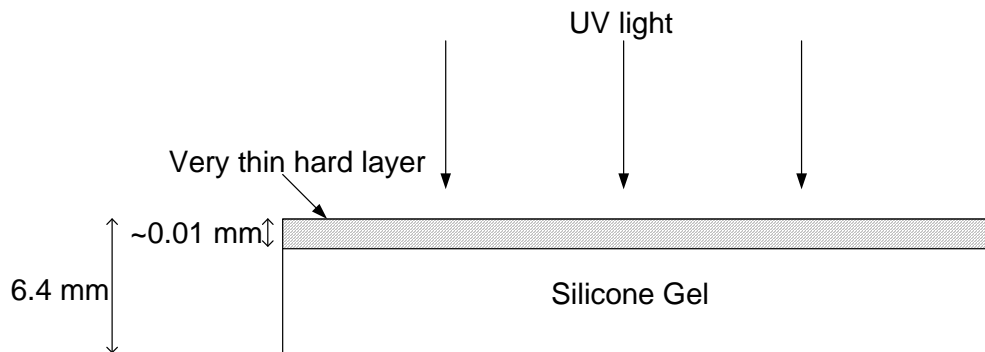


Figure 3-9. Diagram of the hard layer created by UV treatment on the gel (not to scale)

The same vacuum pump used for deforming the silicone gel was used to also help separate the silicone gel and the Fresnel lens by pulling the silicone gel from opposite side of the Fresnel lens.

4 CONSTRUCTION OF THE ILLUMINATION SWITCH

The previous chapter presented the basic concept and design of the illumination switch. In this chapter, details of the construction of the illumination switch and associated challenges and their solutions are described.

4.1 CONSTRUCTION OF THE ILLUMINATION SWITCH

4.1.1 Detailed Design of the Illumination Switch

The illumination switch was composed of a sheet of transparent silicone gel and a converging Fresnel lens. Figure 4-1 shows the schematic diagram of the cross-section of the illumination switch.

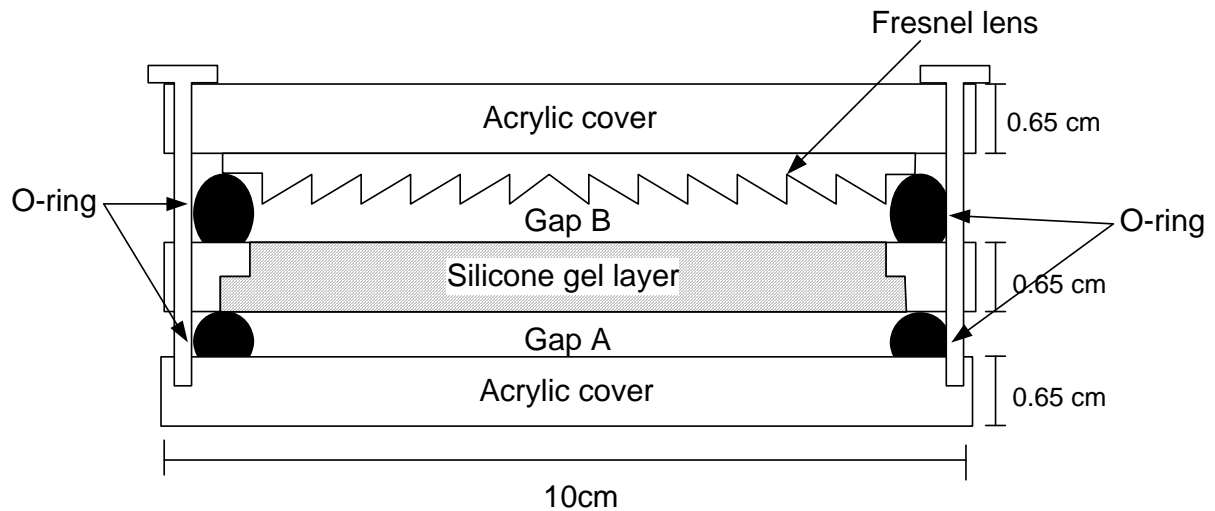


Figure 4-1. Schematic diagram of the cross-section of the illumination switch

The Fresnel lens was positioned adjacent to the silicone gel layer and both were sandwiched between transparent acrylic plates. The Fresnel lens used for the illumination switch was manufactured by Edmund Optics⁵² with a focal length of 7.5 cm and an optically active lens area was 6 cm in diameter. The silicone gel was cast in an aluminum frame which had a circular opening in the middle. The top, bottom, and side views of the aluminum frame are shown on Figure 4-2(a). One of the issues with the cast silicone gel in the aluminum frame

was that the silicone gel separated from the frame when ‘Gap B’ on the Figure 4-1 was vacuumed. This was not a problem when vacuuming ‘Gap A’ because the pressure was not large enough to cause this issue. The maximum pressure applied to Gap A was about -10 kPa but that of Gap B was about -70 kPa which was enough to cause the separation. Once the silicone gel separated from the frame, the gaps on each side of the silicone gel were connected resulting in failure of the deactivation of the Fresnel lens. In order to prevent this problem, the aluminum frame was built to have a counter-bored shape. This counter-bored structure prevented the gel from separating by having half the thickness of the silicone gel layer larger than the other so that pulling the silicone gel from the Fresnel lens side did not cause the separation.

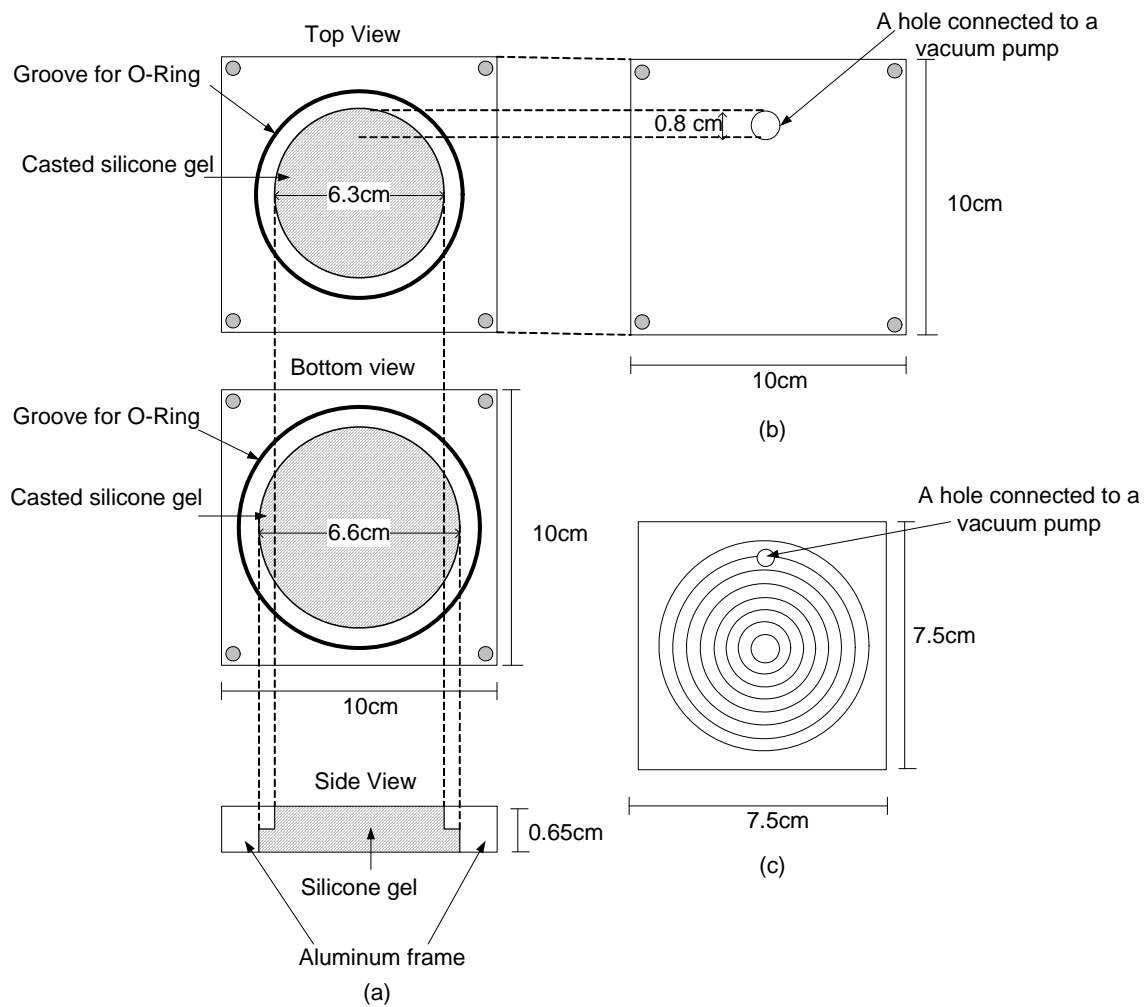


Figure 4-2. Schematic diagrams of (a) the aluminum frame, (b) the acrylic cover, and (c) the Fresnel lens (not to scale)

Figure 4-2 (b) and (c) show the schematic diagram of the acrylic cover and the Fresnel lens. They had a hole for connecting the vacuum pump to the illumination switch. The two acrylic covers, Fresnel lens, and the aluminum frame with silicone gel were held together with four bolts on each corner, and the device was sealed using o-rings.

4.1.2 Air Channel on the Fresnel Lens

Because of the geometry of the Fresnel lens, the air near the outer rings of the Fresnel lens was vacuumed out first and the deformed silicone gel sealed up the vacuumed region from the rest, resulting in trapping the air in the rest of the lens as shown on Figure 4-3 (a).

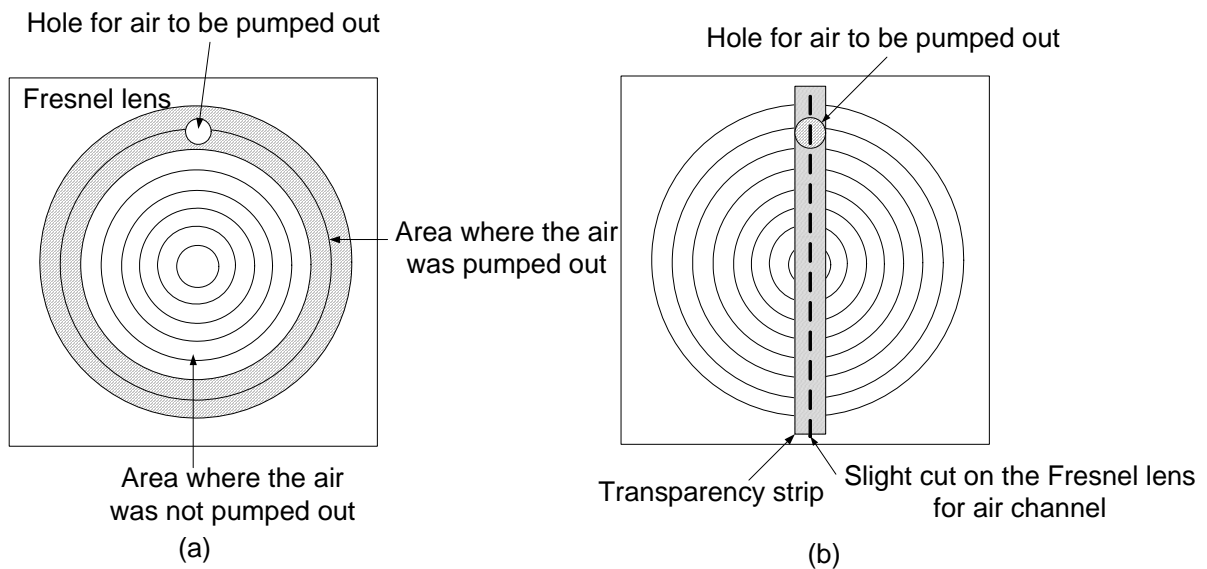


Figure 4-3. A schematic diagram of the Fresnel lens showing (a) the area where the air was pumped out (shaded region) and the area where the air was trapped (not shaded region) and (b) an air channel

This problem was solved by an air channel created on the Fresnel lens as shown in Figure 4-3 (b). This was done by creating a slight cut on the Fresnel lens and covering it with a thin strip of transparency sheet to prevent the silicone gel from deforming into the air channel. A close up view of the side view of this air channel is shown in Figure 4-4.

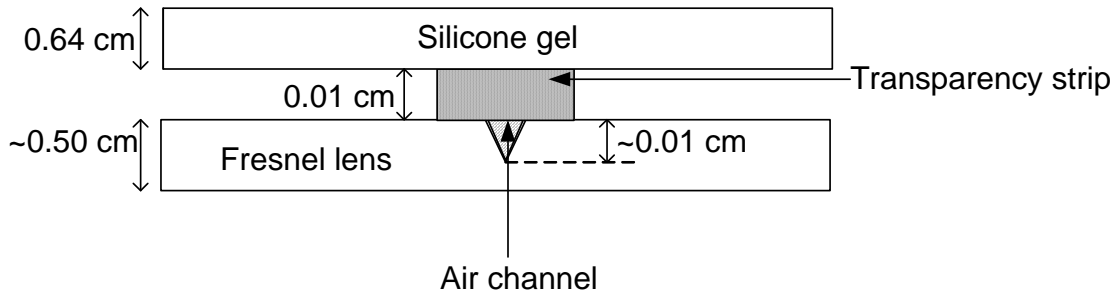


Figure 4-4. A closer look at the air channel on the Fresnel lens (side view, not to scale)

4.1.3 Deformation of the Silicone Gel

In the actual constructed illumination switch, the deformation of the silicone gel was not perfect since it was difficult to perfectly fill the prisms of the Fresnel lens. Figure 4-5 shows the diagram of the perfectly deformed silicone gel and the actual deformation of the silicone gel.

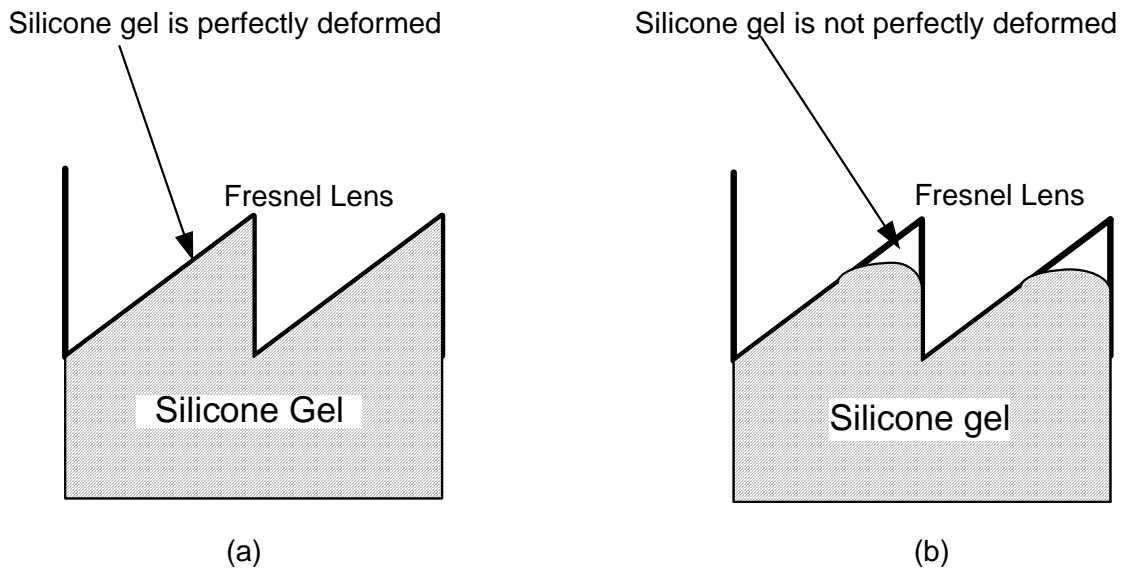


Figure 4-5. (a) Perfectly deformed silicone gel on TracePro and (b) actual deformed silicone gel which is not perfectly deformed

By using a microscope and by looking at the illumination switch from its top when the silicone gel was deformed into the Fresnel lens, it could be estimated how much area of the

Fresnel lens was not filled. The area on the Fresnel lens where the silicone gel was not in contact with the silicone gel was estimated to be about 10 % of the total area of the lens.

4.2 PNEUMATIC COMPONENT OF THE ILLUMINATION SWITCH

In order to deform and restore the silicone gel, a Duo Seal Two-Stage vacuum pump⁵³, was used to pump the air out of the gap. The maximum pressure that this vacuum pump was capable of creating was about -75 kPa. In order to both deform and restore the gel using only one vacuum pump, it was necessary to switch the air flow between each side of the silicone gel to the vacuum pump. The pneumatic component of the illumination switch was designed so that it could change the air flow from one side of the silicone gel to the other. A solid state relay⁵⁴, two and three way valves, and a function generator were used for the pneumatic part of the illumination switch.

A pneumatic valve is a device that controls and regulates the flow of gas or fluid. For the pneumatic component of the illumination switch, a 3/2 way valve and two 2/2 way valves were used. 3/2 way valves had three openings; two inlet ports and one outlet port. This valve could change the air flow in one direction to the other and the 3/2 way valve⁵⁵ used was a normally-closed solenoid valve. As shown in Figure 4-6, the left inlet was open when the valve was not energized and the right inlet was closed so the air flows from the left inlet to the outlet port. When the valve was energized, the left inlet closed and the right inlet opened so the air flows from right inlet to the outlet port.

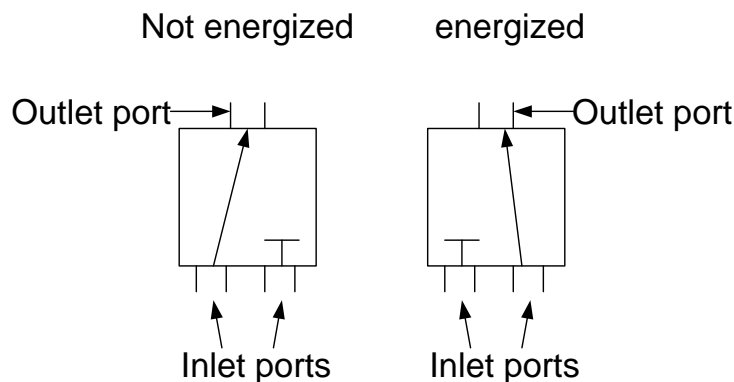


Figure 4-6. Diagram of the 3/2 way valve showing the air flow

2/2 way valves had two openings; one inlet port and one outlet port. The 2/2 way valve⁵⁶ used was a normally-closed solenoid valve which controlled the flow of air by running or stopping an electric current through a solenoid to open and close the valve as shown in Figure 4-7.

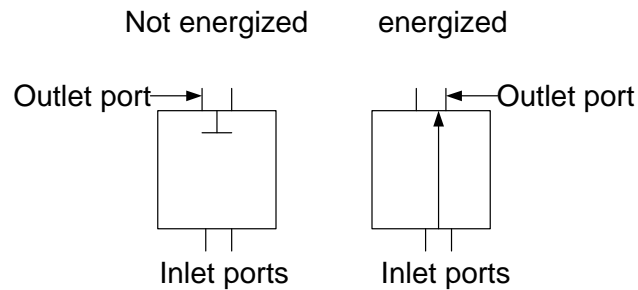


Figure 4-7. Diagram of the 2/2 way valve showing the air flow

Figure 4-8 shows the schematic diagram of the pneumatic component of the illumination switch. Each side of the illumination switch was connected to a 2/2 way valve and a 3/2 way valve, and then a vacuum pump. The 3/2 way valve and 2/2 way valves were connected to a solid state relay and a function generator which controlled the valves. All the valves were normally closed and they were open when they were energized. The speed of the switching cycles was controlled by a frequency and duty free cycle of the function generator.

When the function generator provided 5 V, side A on the solid state relay was activated and turned on the 3/2 way valve and one of the 2/2 valves on the Fresnel lens side so that the silicone gel was deformed into the shape of the lens to deactivate the Fresnel lens as shown in Figure 4-8 (a). At this time, the 2/2 way valve of the silicone gel side was closed and the one on the Fresnel lens side was open, so air from the gap between the Fresnel lens and the silicone gel was pumped out.

When the function generator provided -5 V, the 2/2 valve on the silicone gel side was switched on and the other valves were switched off as shown on Figure 4-8 (b). In this case, the air flows from the back of the silicone gel, so the gel was pulled from the back to help separate the lens and silicone gel.

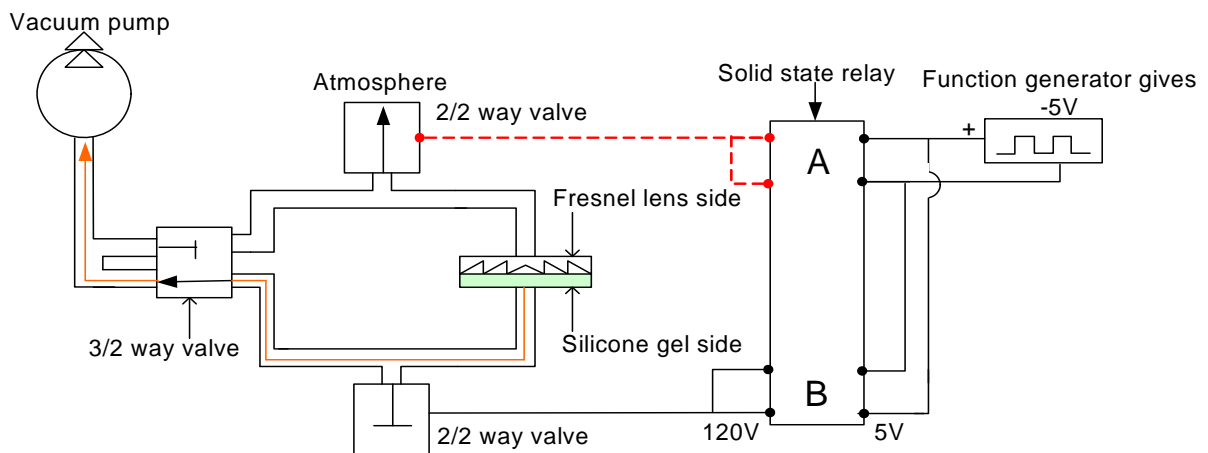
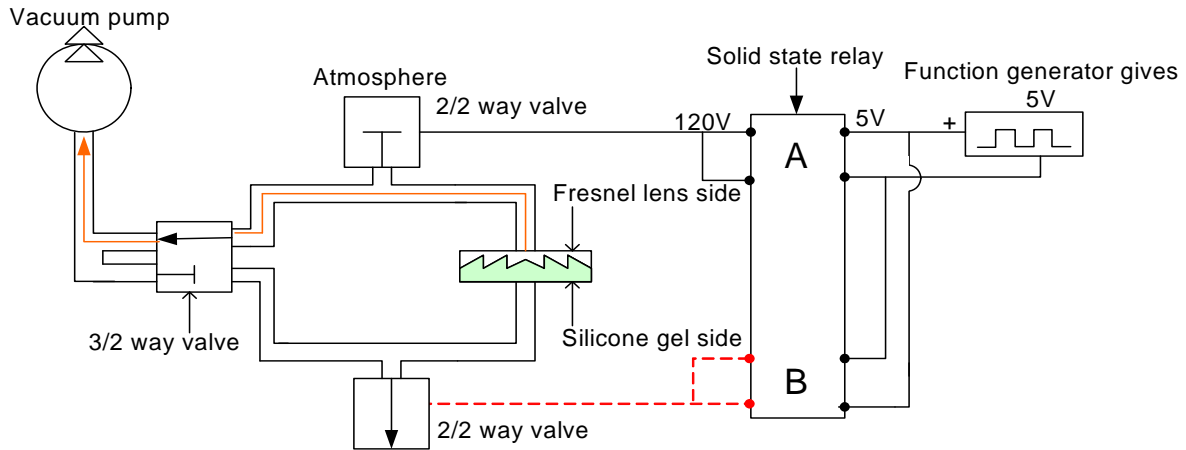


Figure 4-8. Schematic diagram of the pneumatic part of the illumination switch

An illumination switch using the Fresnel lens, silicone gel, and the pneumatic switch was successfully constructed, and the performance and endurance of this device was measured, as is presented in the next chapter.

5 EXPERIMENTAL RESULTS

In this chapter, the experimental methods required to evaluate the performance of the constructed illumination switch and their results are presented.

5.1 METHODS OF MEASUREMENT

The performance of the constructed illumination switch was evaluated using the measurement approaches described in this section.

5.1.1 Integrating Detector

An integrating sphere is often used to measure the intensity of light in optics⁵⁷. Instead of a spherical shape, the integrating detector had a cylindrical shape, as shown in Figure 5-1 as it was easier to construct and errors introduced by the deviation from a spherical shape were not substantial. The integrating detector had an opening of 2 cm in diameter for the light to enter the detector. The opening represented 2.4 % of the total surface area, as long as it is less than ~5 % of the total, it still works as an effective integrating structure⁵⁸. A schematic diagram of the integrating detector is presented in Figure 5-1.

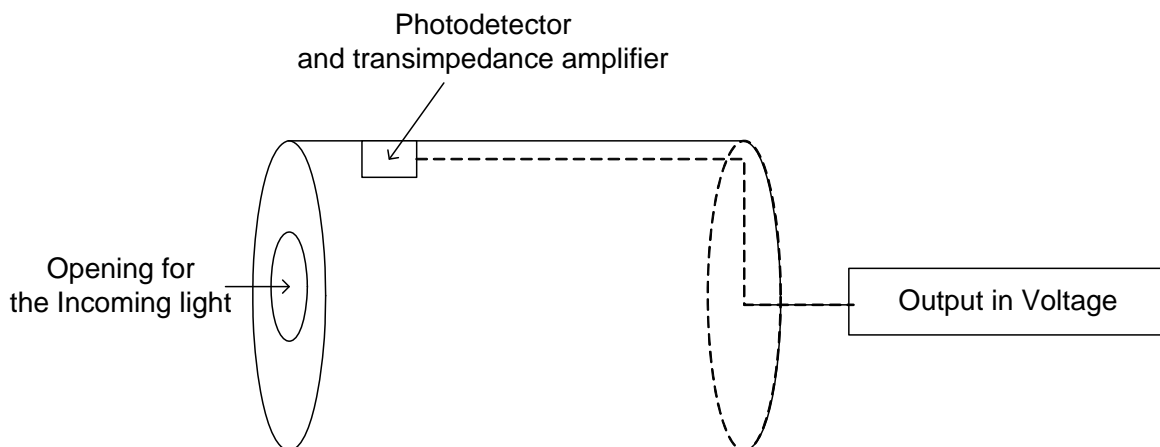


Figure 5-1. Schematic diagram of the integrating detector

The integrating sphere detected light and measured its intensity using a light-to-voltage converter⁵⁹ which consisted of both a photodiode and transimpedance amplifier to detect the intensity level and converted it to a voltage.

This integrating detector was capable of outputting a voltage that varies linearly with the intensity of light, the provided output was within the range between 0.5 and 4 V. Throughout all the measurements in this project, neutral density filters were often used as necessary in order to reduce the light intensity to obtain output voltages within this range. The neutral density filters reduced the light intensity uniformly at all wavelength and transmittance of the filter was taken into account. An infrared filter⁶⁰ was also inserted in front of the integrating detector in order to prevent the infrared radiation from entering the detector. This approach ensured that the voltage output of the detector was linearly proportional to the visible light entering the integrating detector.

The measurement set-up consisted of a light source, the illumination switch, integrating detector, and pressure sensors (shown in Figure 5-2). The light source was located a distance of 15 cm away from the illumination switch which was connected to a vacuum pump. The pressure within the gap on either side of the gel was measured using pressure sensors. The output of the pressure sensors and integrating detector were connected to a data acquisition card and the measured values were recorded by a LabView program from National Instruments⁶¹. The integrating detector was located at the focal point of the Fresnel lens where the transmitting devices would have been obtaining light for illumination.

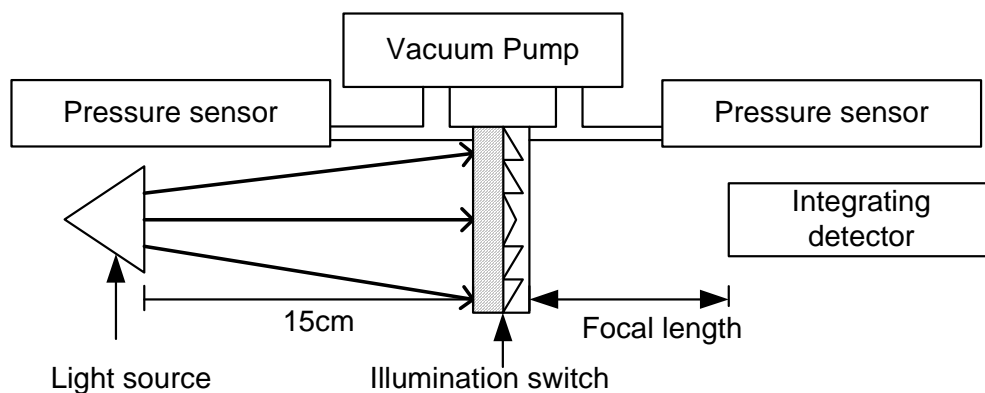


Figure 5-2. Schematic diagram of the optical part of the measurement system

There were mainly two different factors that were calculated by using the intensity level measured by the integrating detector. One was the “relative intensity” which was calculated by:

$$\text{Relative intensity (\%)} = \left(\frac{\text{Measured intensity}}{\text{Intensity at 0kPa when the device is active}} \right) \times 100 \quad (5.1)$$

The other was the “change in intensity” which was calculated by:

$$\text{Change in intensity (\%)} = 100 - \text{Relative intensity} \quad (5.2)$$

All the errors for the measured intensities came from the reproducibility of the measurements (mainly from misalignment of the measurement set-up), which was estimated to be about 3% of the measured intensity.

5.1.2 Producing a Collimated Beam

In order to produce a collimated beam of light for testing purposes, a commercially-available reflector lamp with a full beam angle of 38° (half angle of 19°) was used. This amount of beam spread was consistent with the maximum anticipated sunlight collimation half angle of 20°.

The angular output distribution of the light source was measured experimentally. This was accomplished by positioning the light source at a distance 160 cm away from a measurement surface, and measuring the illuminance on the measurement plane at 10 cm intervals along a line that passed through the peak of the distribution, and the divergence angle, θ , was calculated for each measurement position relative to the surface normal of the measurement plane, as shown on Figure 5-3.

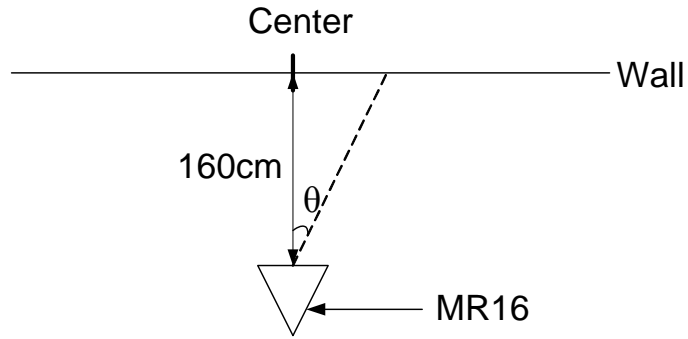


Figure 5-3. Diagram showing the angle θ

Figure 5-4 shows the relative intensity level as a function of the divergence angle. The relative intensity was calculated as the ration of the measured illumination at a given position to the peak illuminance, at $\theta = 0^\circ$.

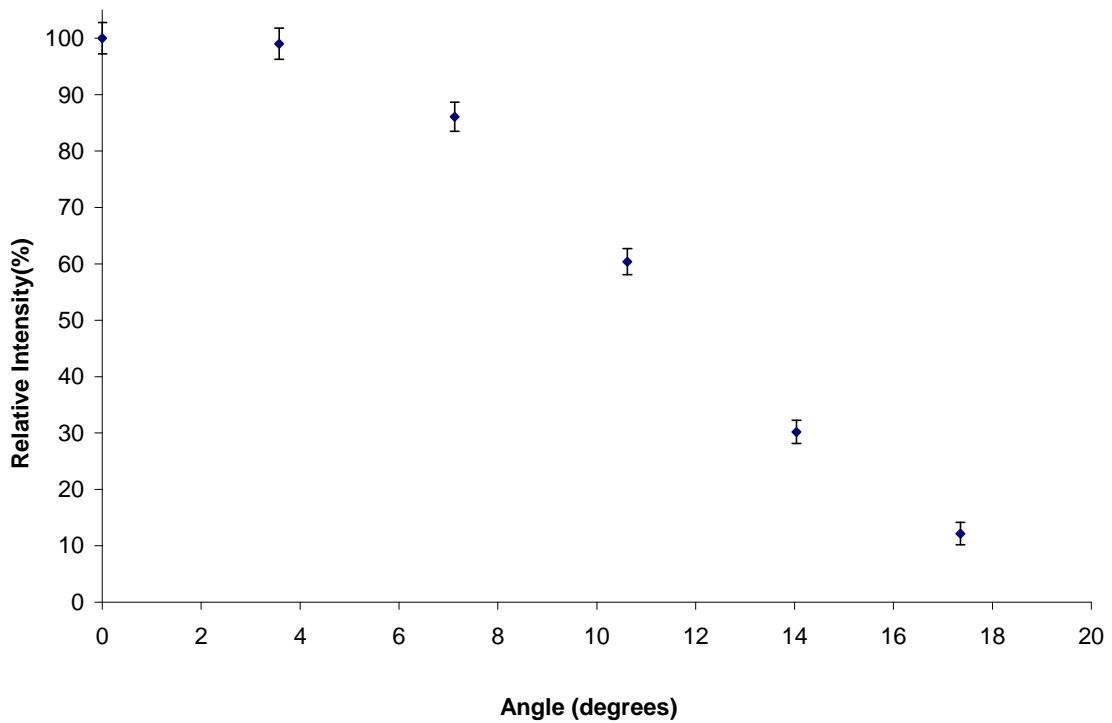


Figure 5-4. Intensity distribution of light source

5.1.3 Measuring the Pressure

In order to measure the pressure on either side of the silicone gel, two integrated silicon pressure sensors⁶² were used. These sensors measured the pressure relative to atmospheric pressure and outputted a corresponding voltage. They were capable of measuring pressure in the range of -115 to 0 kPa. The measured voltage could be converted to pressure in kPa by using:

$$P(kPa) = \frac{\frac{V_{out}}{V_{source}} - 0.92}{0.007652} \quad (5.3)$$

where V_{out} is the measured voltage and V_{source} is the source voltage used for the pressure sensors. The output of the pressure sensors were connected to a data acquisition card along with the integrating detector so that the pressure and intensity of light at the focal point of the Fresnel lens could be measured simultaneously.

5.2 HYSTERESIS OF THE SILICONE GEL

The hysteresis effect due to the stickiness of the non-UV treated silicone gel surface was confirmed by measuring the intensity of the light at the focal point of the Fresnel lens as the silicone gel was pushed into and released from the lens surface. The experimental results are shown in Figure 5-5, where the x-axis indicates the applied pressure on the gap between the Fresnel lens and the silicone gel relative to the ambient pressure, and the y-axis indicates the relative intensity at the focal point calculated by using equation (5.2). The illumination switch was initially focusing the light, so the relative intensity was 100 % at 0 kPa on the “Increasing Pressure” data set. As the pressure was increased in the negative direction (i.e. vacuum), the relative intensity decreased to about 40 %. The vacuum was then slowly removed as indicated by the “Decreasing Pressure” data set. For the “Increasing Pressure” data set, each measurement was recorded about 10 seconds after the pressure was changed which was enough time for the intensity to stabilize. However, for the “Decreasing Pressure” data set, each measurement was recorded 60 seconds after the pressure was changed because

the silicone gel did not separate as quickly from Fresnel lens but it took about 50 to 60 seconds until the intensity measurement has stabilized.

As indicated by the results, the intensity did not return to the initial value for each pressure reading, suggesting that the gel remained. When the applied pressure reached 0 kPa, the relative intensity stayed at about 80 % and did not return back to 100 %. Visual inspection of the device showed that a small area of the silicone gel was still in contact with the Fresnel lens and did not separate completely. This behavior was the reason why UV treatment was necessary for the illumination switch.

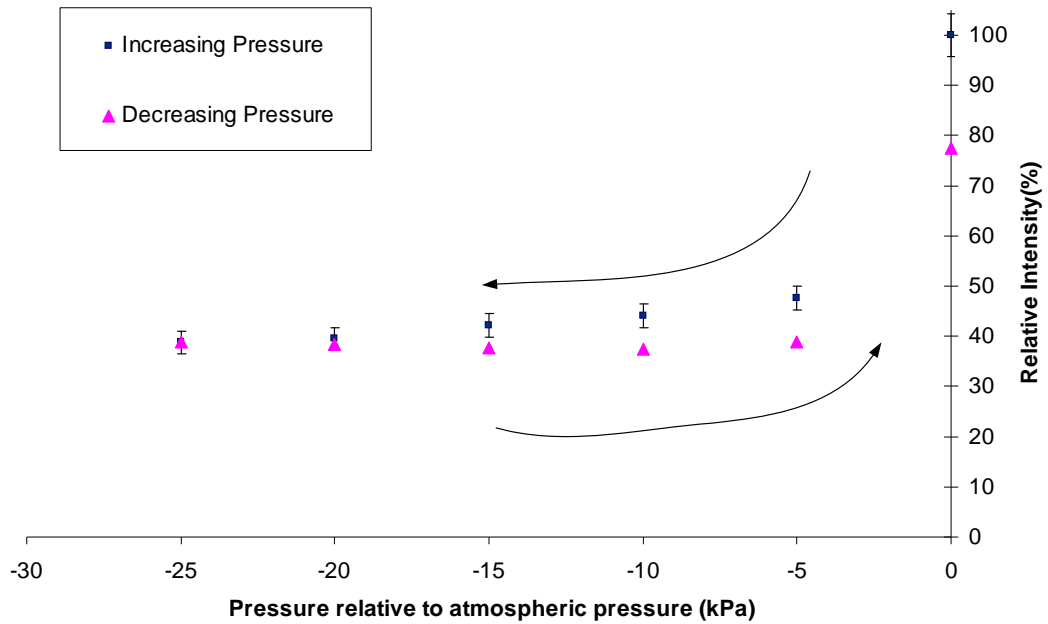


Figure 5-5. Hysteresis of the silicone gel in the illumination switch

5.3 INTENSITY CHANGE WITH AMOUNT OF UV TREATMENT

As discussed in Chapter 3, the UV treatment of the silicone gel surface was used to prevent the surface from being sticky. The UV lamp used in this project was from Dymax⁶³ with a mercury light bulb⁶⁴ which had a spectral intensity distribution shown in Appendix A. In order to optimize the change in intensity using this device, it was necessary to determine the

amount of sufficient UV treatment since too much UV treatment would make it difficult for the gel to deform into the Fresnel lens. In order to decide how much UV treatment was needed, the change in intensity was measured using silicone gels with different UV treatment duration. The UV treatment durations used for the silicone gels were 0, 15, 30, 60, and 120 min. The graph showing the change in intensity is shown in Figure 5-6. The x-axis shows the pressure within the gap between the silicone gel and the Fresnel lens relative to atmospheric pressure (where negative relative pressure indicates vacuum) and the y axis shows the change in intensity at the focal point.

The maximum change in intensity caused by the non-UV treated silicone gel forced into contact with the lens was about $75 \pm 1.0 \%$ at -50 kPa. As the UV treatment time increased, the pressure needed to reach the maximum change in intensity also increased. On the other hand, the change in intensity was smaller for silicone gels with more UV treatment. For example, using the silicone gel with 120 min UV treatment gave only up to $55 \pm 1.7 \%$ change in intensity. It was concluded that 30 min of UV treatment was the optimal amount since the maximum change in intensity was still the same as the untreated gel and the required pressure to reach the maximum intensity was about -60 kPa which was only slightly more than without any UV treatment. The silicone gel with 30 minutes of UV treatment separated from the Fresnel lens easily and the change in intensity was the same as was measurement without any UV treatment.

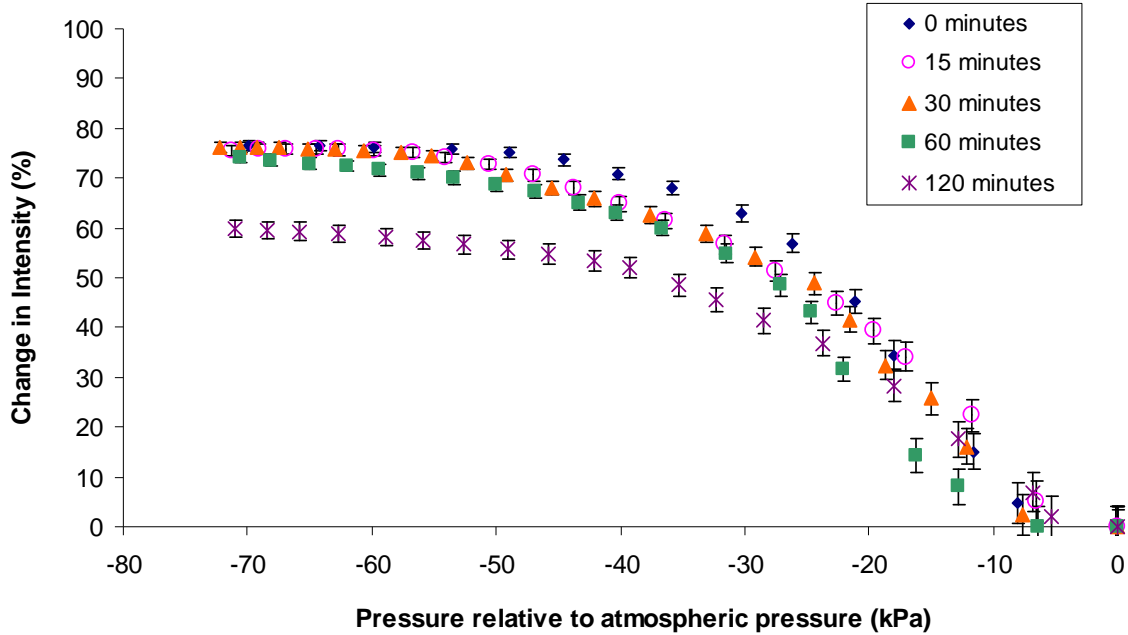


Figure 5-6. Change in intensity using silicone gels with different duration of UV treatment with $f=7.5$ cm Fresnel lens

5.4 MEASURING THE RELATIVE ADHESIVENESS OF THE SILICONE GEL WITH DIFFERENT UV TREATMENT TIME

In order to better understand how the UV treatment time using the particular UV lamp used in this experiment on the surface of silicone gel influenced the stickiness of the gel, an experiment measuring the relative adhesiveness of the gel with different UV treatment times was conducted. Many adhesive product manufacturers examine the adhesiveness of their products with various tests. One example of accurately measuring the adhesiveness is to use a pull-off test. Common pull-off adhesion testers involve pushing a small ball into an adhesive surface with a known force and then measuring how much force is required to completely separate the ball from the adhesive⁶⁵. A modified version of this test was conducted using a small ball rolling on an inclined plane formed by the adhesive layer. The terminal velocity of the ball, or the maximum speed achieved by the ball, rolling down the incline was measured for silicone gels with different UV treatment times. The schematic diagram of the set up for the adhesion test is shown in Figure 5-7(a). A piece of silicone gel

with a size of about 5 cm × 5 cm was placed on a 20° inclined slope, and a video camera was placed just beside the incline so that it videotapes the ball coming from the top to the bottom of the incline. Once the video camera recorded the motion of the ball, Logger Pro program⁶⁶ was used to analyze the position and the speed of the ball at a given time. By manually locating the position of the ball (red dots in Figure 5-7(b)) at different times throughout the recorded video, the program determined the position (x and y direction indicated on the figure) of the ball at each time.

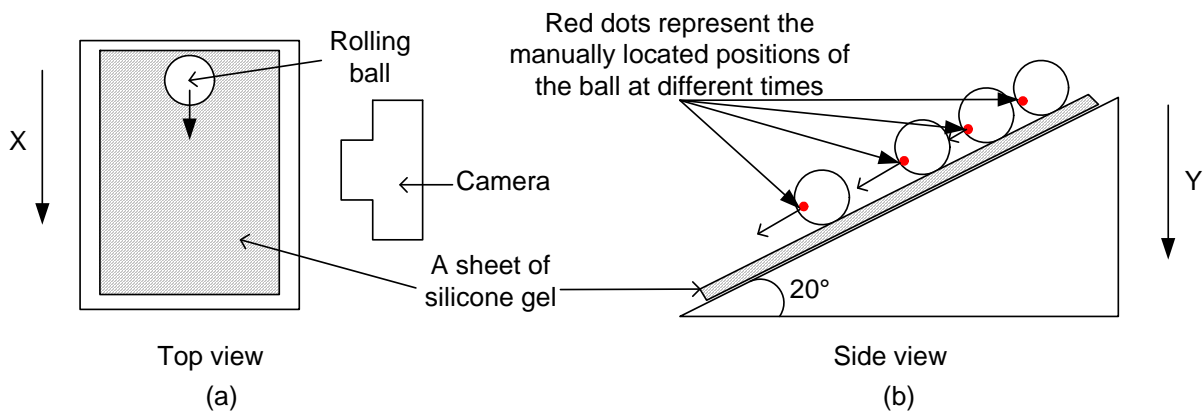


Figure 5-7. Set up of the relative adhesion test

As an example, Figure 5-8 shows the acceleration of the ball when silicone gel was UV treated for 15 minutes. Although there were some fluctuations, it was clear that the acceleration of the ball initially increased, then started to decrease at around 1.2 seconds and reached zero close to 1.4 seconds.

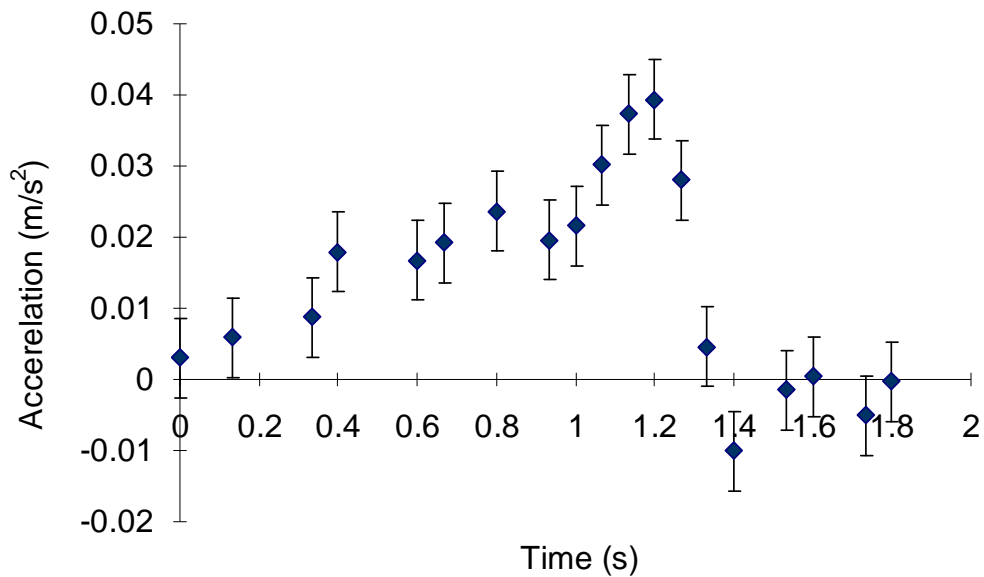


Figure 5-8. Acceleration of the ball

Once the time it took for the ball to reach the acceleration was determined, the terminal velocity of the ball was calculated. It was done by first taking the slope of the position graph on each coordinate after the ball reached zero acceleration as shown in Figure 5-9, which was the velocity of the ball after it reached the terminal velocity. Then using these velocities in x and y directions, the terminal velocity was calculated by:

$$V_{\text{terminal}} = \sqrt{(V_x)^2 + (V_y)^2} \quad (5.3)$$

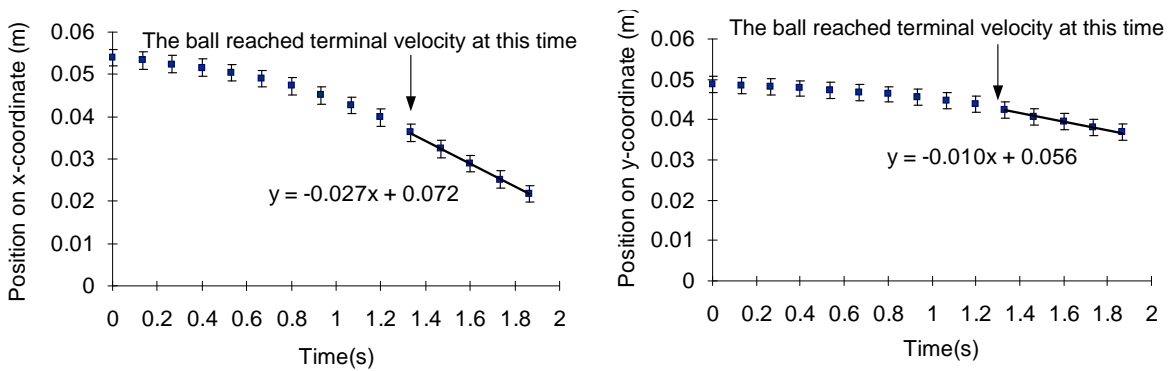


Figure 5-9. Graphs of x and y positions of the ball as a function of time

Using this method, the terminal velocity of the ball on silicone gels with different UV treatment times was determined, and the results are shown in Figure 5-10. The terminal velocity seems to increase almost linearly with respect to the UV treatment time, which was not surprising since it may indicate that over a certain range of UV treatment times, the thickness of the hard surface layer depends proportionally on the duration of the treatment.

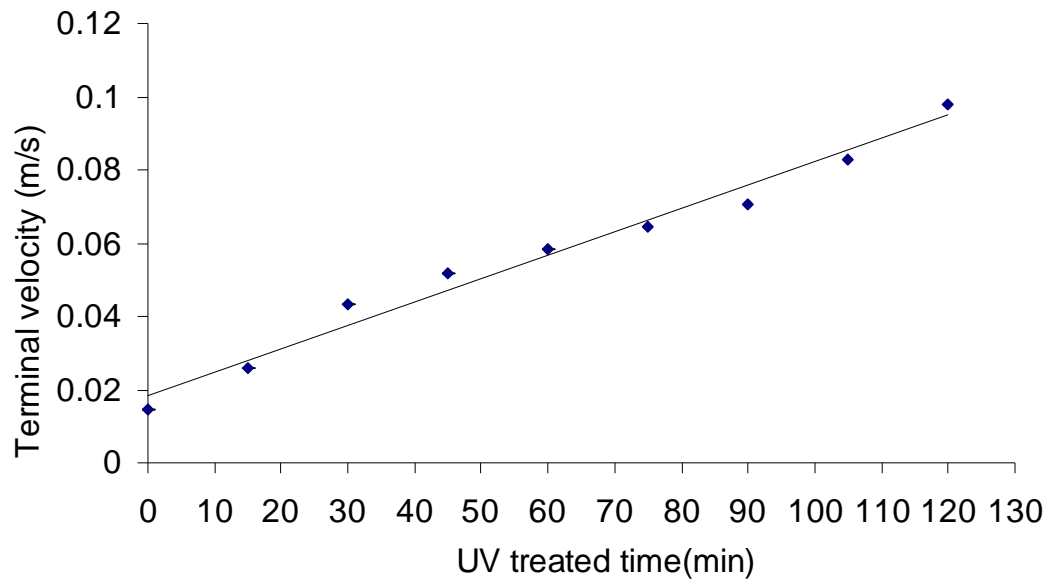


Figure 5-10. Adhesion of the silicone gel with various UV treatment times

5.5 UV TREATMENT ON THE SURFACE OF THE SILICONE GEL

When the silicone gel was UV treated for a long time (more than 3 hours), it was possible to visually see a difference in the surface of the gel, and it was reasonable to assume that this was a result of the formation of a hard surface layer. Consequently, it was appropriate to observe this surface more closely. For many surfaces, a scanning electron microscope (SEM) would be used to investigate the surface properties. However, it is well known that soft materials are difficult to examine with SEM because they usually contain substances that evaporate under high vacuum, such as water or oil⁶⁷ which prevent the sample from being uniformly conductive which result in poor imaging under the SEM. Soft samples usually

require special preparation beforehand, such as Cryo-SEM⁶⁸, where the sample is frozen before scanning under SEM. Another approach for soft materials is to use an environmental SEM (ESEM) which does not require high vacuum and the sample does not have to be conductive. This is a very powerful method of understanding structures of soft materials nowadays^{69,70}. Since there was a concern that Cryo-SEM preparation would ruin the structure of the silicone gel by cracking the surface, ESEM was used to image the silicone gel. Two samples were prepared for ESEM imaging, one sample with no UV treatment and a second with four hours of UV treatment. Both of the samples were cleaved into smaller pieces (about 4×4 mm) as shown in Figure 5-11 (a), and the cleaved surfaces (indicated by the shaded regions in Figure 5-11) were examined under the ESEM. As the pictures in Figure 5-11 (b) shows, the silicone gel without UV treatment had a very smooth surface everywhere. On the other hand, the surface of the silicone gel with four hours of UV treatment looked very rough near the UV treated surface. It was suspected that these cracks were caused by when the silicone gel was cut with a knife. This result suggests that there was a hard layer created by the UV treatment and this surface could be damaged (i.e cracked) by the tip of the prism of the Frsnel lens while the silicone gel is deformed into the lens. The cracks might cause the inner silicone gel to come out to its surface. This would make the surface of the silicone gel sticky again and stop separating from the lens once the gel is in contact with the lens. Hence, an experiment for checking if this was an issue after switching the illumination switch for a number of times was done which is presented in the next section.

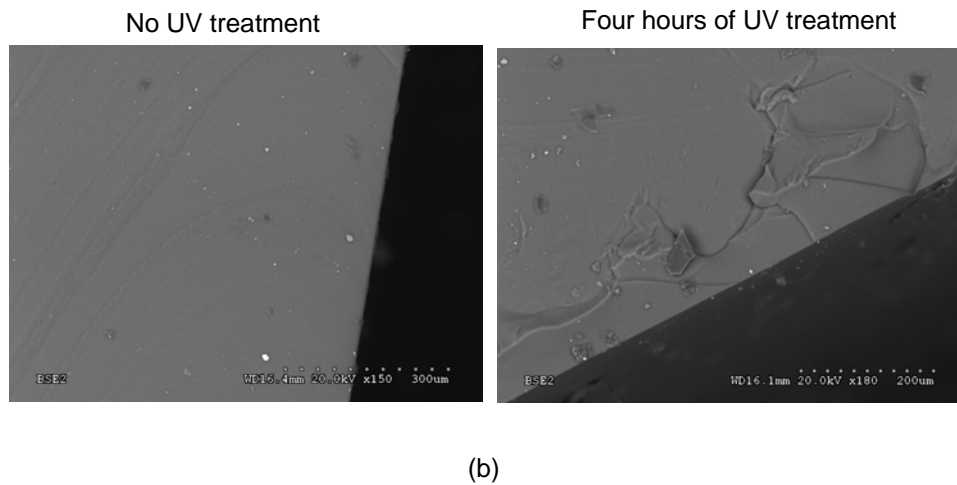
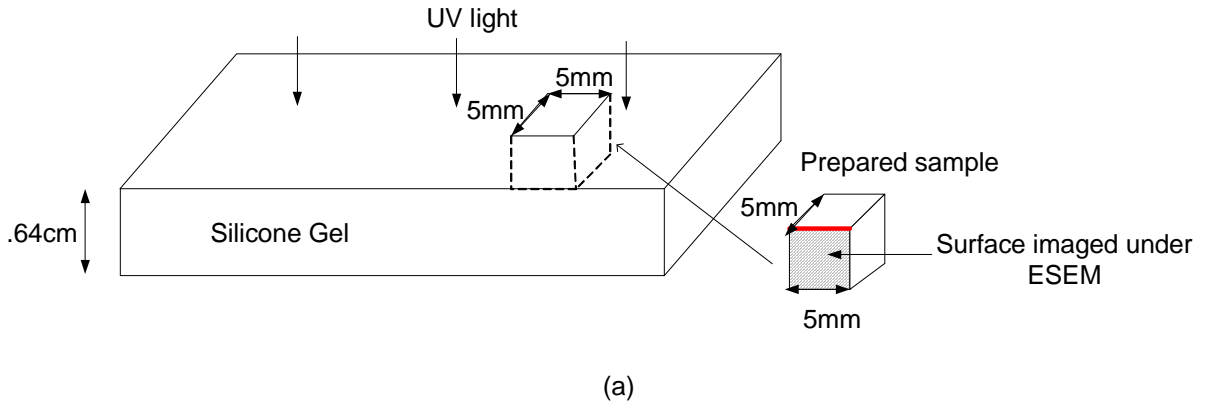


Figure 5-11. (a) Diagram of the sample silicone gel and (b) ESEM images of the gel without UV treatment and after four hours of UV treatment

5.6 ENDURANCE OF THE ILLUMINATION SWITCH

It is important to check the endurance of the illumination switch in order to test the suitability of the device in the real world application. In this section, the experiments for measuring the degradation of the performance with respect to the number of switch cycles and also under low and high temperature environments are presented and discussed.

5.6.1 Endurance of the Device After Many Switch Cycles

The performance of the illumination switch was tested to confirm that the device could be activated and deactivated many times without degradation in its performance. In this

experiment, one switch cycle consisted of increasing the pressure up to -50 kPa, waiting for 5 seconds, and then decreasing it to 0 kPa. The pressure changes were achieved in about 0.2 seconds. Figure 5-12 shows a typical example of one switch cycle. This figure shows high and low level illumination and the combination of those two states were defined as one switch cycle.

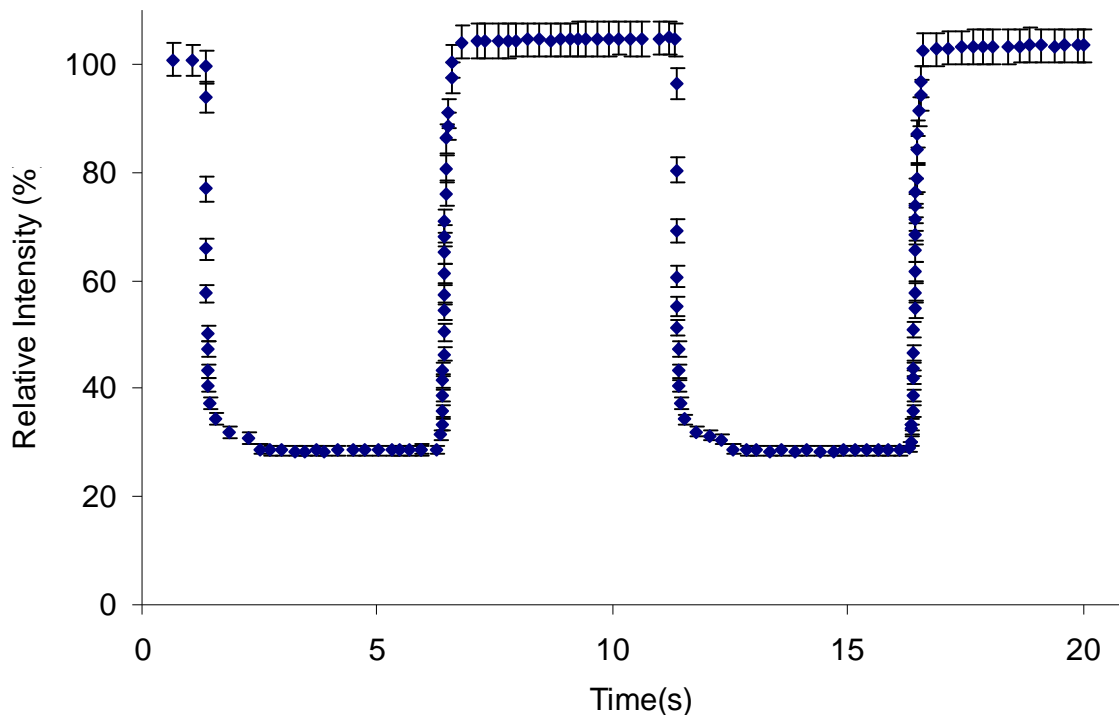


Figure 5-12. A typical example of one switch cycle

The illumination switch was operated for 3000 switch cycles and its performance was evaluated by measuring the change in intensity at the focal point of the lens, as well as the length of time required for the gel to separate from the lens. This number of switch cycles, was chosen since the experiment required about 5 days and it was considered that this was a reasonable number of cycles for this preliminary experiment.

As Figure 5-13 shows, the change in intensity of the illumination switch was unchanged over 3000 switch cycles. Intensity change was 72 ± 2.0 % for the first switch and it was the same within error throughout.

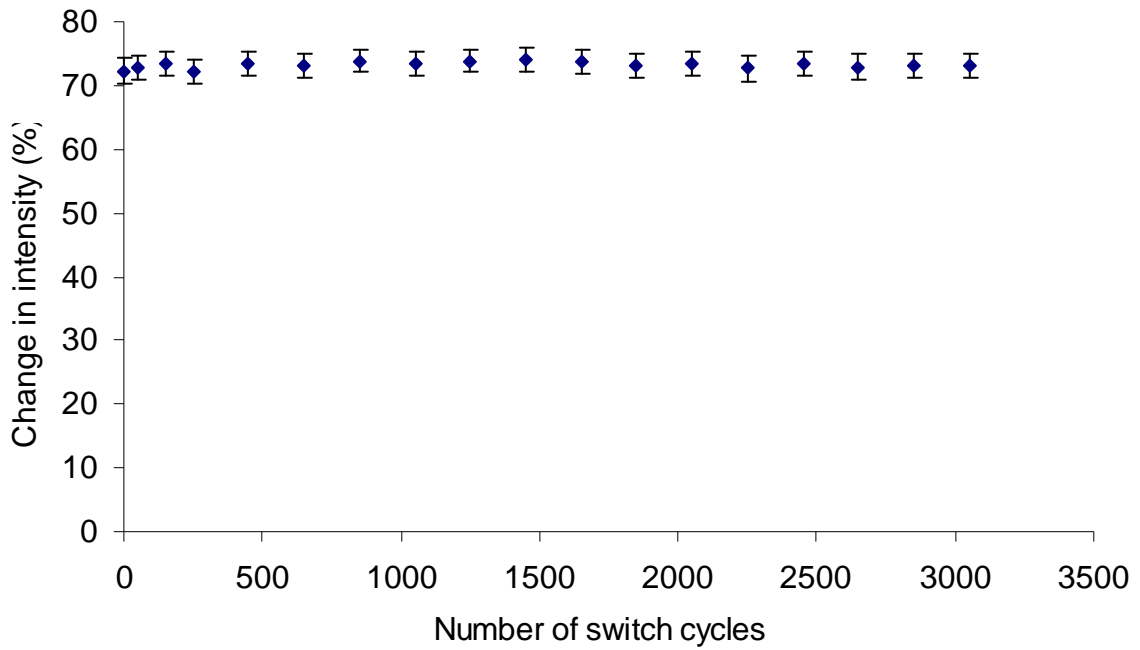


Figure 5-13. Endurance test due to the number of switch cycles

It was also a concern that the prisms of the Fresnel lens may break the thin hard surface of the silicone gel causing the interior sticky gel material to make contact with the lens, and therefore require more time and/or pressure for the two surfaces to separate. However, this appeared not to be a problem since as shown in Figure 5-14 the separation time was not changed (within experimental error) between the first switch and the 3000th switch.

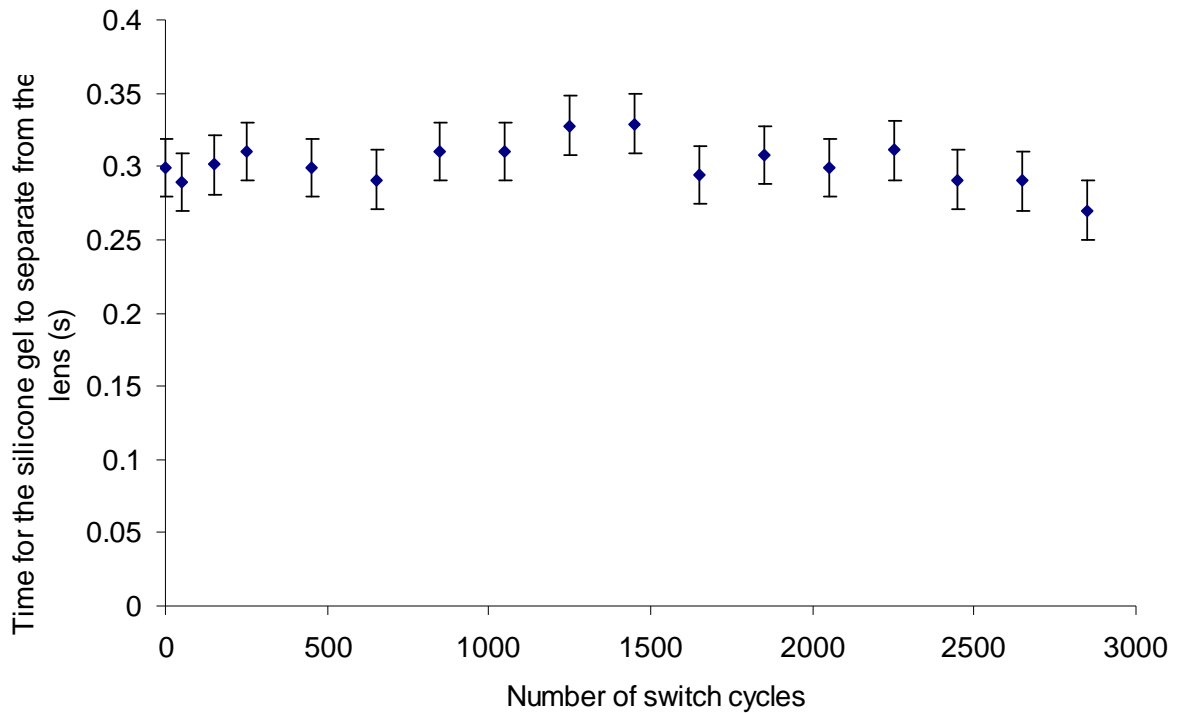


Figure 5-14. Time for the gel to separate from the lens

5.6.2 Endurance Under Different Temperature Conditions

The performance of the illumination switch was also tested under different temperature conditions. The lowest temperature tested was 10 °C since it was anticipated that this would be the minimum required operating temperature inside a light guide and similarly the highest temperature anticipated inside a guide was about 60 °C. The following sections presents the cooling and heating systems used for this test and their results.

5.6.2.1 Lower temperature test

Liquid nitrogen was used to cool down the environment of the illumination switch to 10 °C inside a transparent acrylic box enclosing the device, as depicted in Figure 5-15. The acrylic box was connected to an insulated tube which carried the stream of cold nitrogen gas from the liquid nitrogen container. The liquid nitrogen container had two power resistors in parallel (in order to produce more power than when only one resistor was used) which

radiated heat so that liquid nitrogen was evaporated. The two resistors were connected to a power supply which supplied voltage to the resistors. The radiated heat from the resistors changed depending on the supplied voltage so that the temperature inside the acrylic box could be controlled by the power supply.

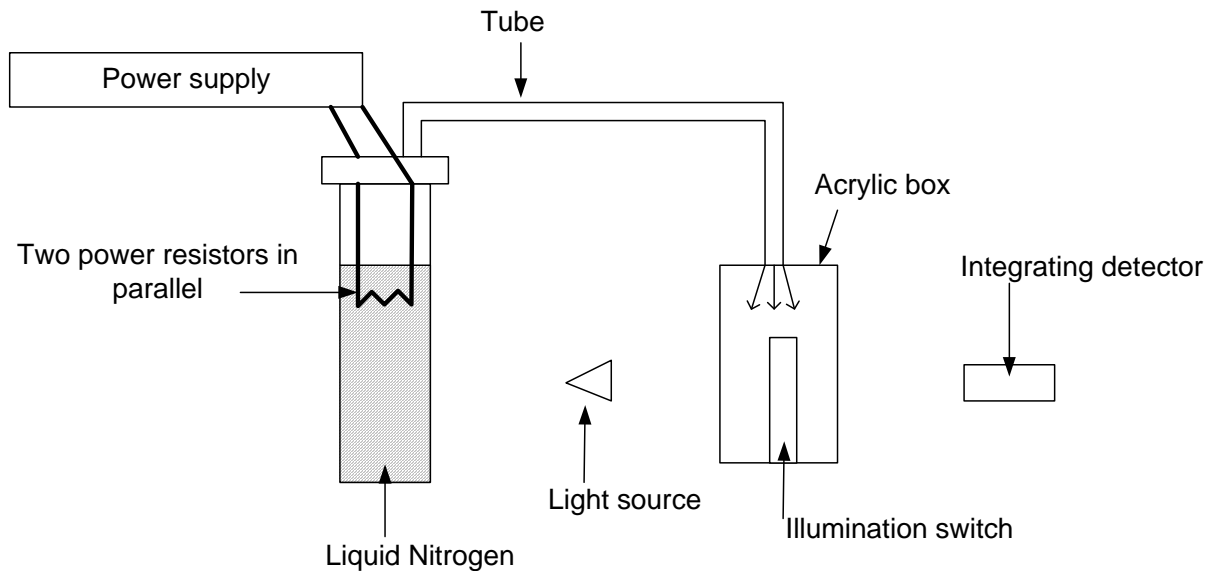


Figure 5-15. Set up for lower temperature test

Using this system, the temperature of the environment of the illumination switch was cooled down to 10 °C. This illumination switch originally changed intensity of light at the focal point of the Fresnel lens by 69.4 ± 2.2 % at room temperature (~ 24 °C). The temperature inside the box gradually decreased and reached 10 °C after about 35 minutes. Then the temperature was maintained at 10 ± 1 °C for an hour. As shown in Figure 5-16, the change in intensity of the light at the focal point did not change over the hour, indicating that the device functions properly at 10 °C.

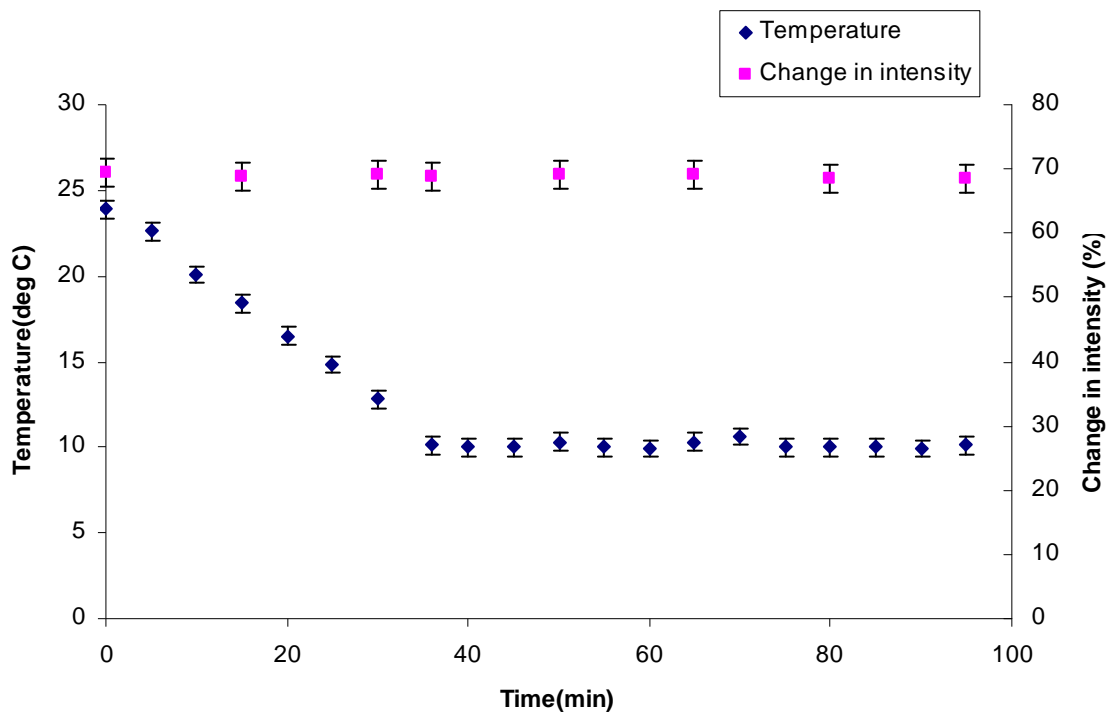


Figure 5-16. Change in intensity of the illumination switch and temperature within the acrylic box with respect to time

Figure 5-17 shows the relative intensity at the focal length as a function of pressure relative to the atmospheric pressure at different temperatures and times. This graph also shows that the way it changed the illumination level of the switch did not change for temperatures at 10 and 24 °C or over 60 minutes at 10 °C.

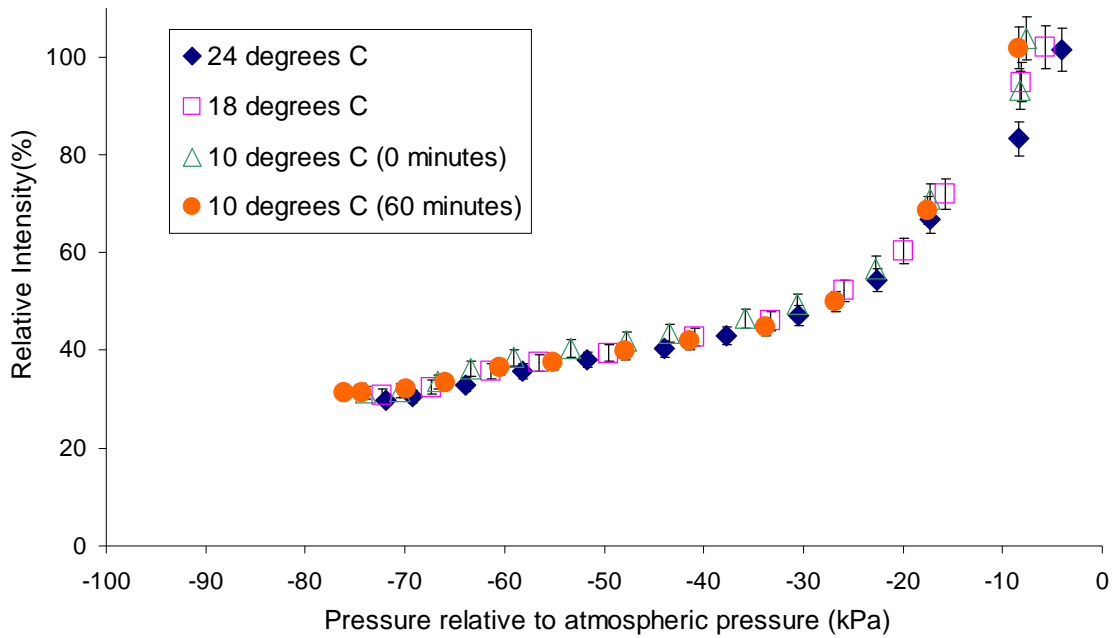


Figure 5-17. Relative intensity vs. pressure graph for lower temperature test

5.6.2.2 Higher temperature test

The illumination switch was also tested in a higher temperature environment. Figure 5-18 shows the side view of the set-up used to create 60 °C environment for the illumination switch. The illumination switch was inside the acrylic box with an open end facing a heater so that hot air could flow into the acrylic box and maintained the desired temperature.

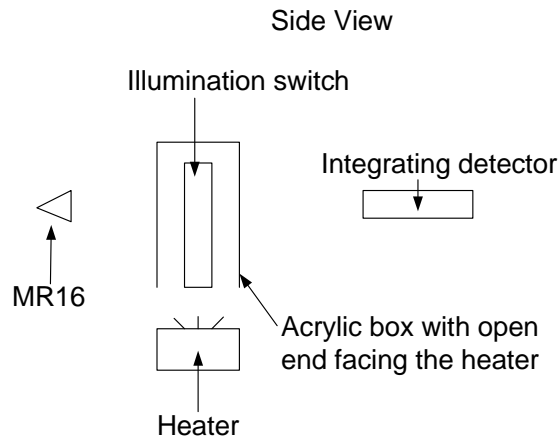


Figure 5-18. Set up of the higher temperature test

When the silicone gel was heated up, it was expected to be more flexible, so it was expected that the device would achieve the same change in intensity without degradation. However, it was postulated that the gel may become stickier and would not separate easily from the lens, even after the pressure is released. Figure 5-19 shows the temperature and the change in intensity of light at the focal point of the lens as a function of time. The temperature was increased to about 60 °C and then maintained between 60 and 65 °C for an hour. As was expected, the change in intensity at the focal point did not change over higher temperatures. Also, visual examination of the illumination switch showed that the silicone gel successfully separated from the Fresnel lens which means that the illumination switch functions well at 60 °C.

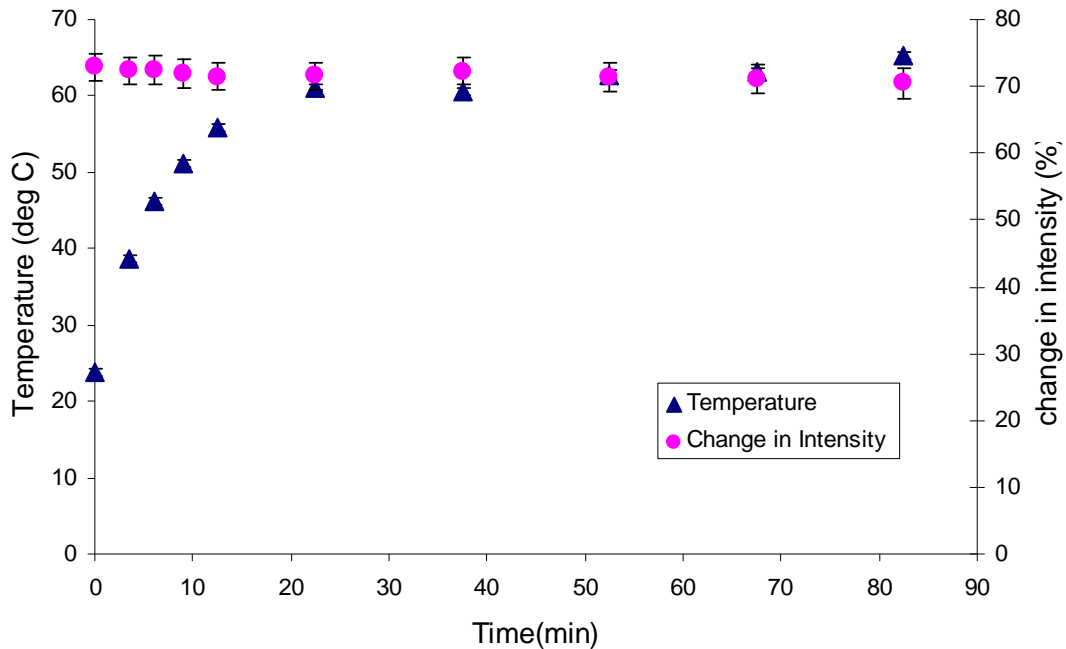


Figure 5-19. Temperature and change in intensity as a function of time for higher temperature experiment

6 RAY TRACE MODELING

In optics, it is useful to conduct ray trace modeling of the experimental set up and compare its result with experimental result. Ray tracing programs simulate behavior of light rays, such as reflections and refractions. In this project, a ray tracing program called TracePro®⁷¹, which employed Monte Carlo simulation technique, was used.

6.1 MODELING WITH A MONTE CARLO RAY TRACING SOFTWARE

Computational ray tracing is a powerful tool for simulating light rays at each interface of both optical and non-optical components since it allows one to understand detail behavior of light rays which is often difficult to do visually. The most straightforward computer ray tracing can be done by using a method called deterministic algorithm. It uses all the initial rays, figures out what each ray does at each interface, then makes a history of these rays for output. On the other hand, Monte Carlo method uses statistic and probabilistic selection of initial rays, then simulates and makes ray histories of these input rays. The Monte Carlo method is often used for ray tracing in optics since it reduces the simulation time significantly compared to other methods and it is also capable of simulating complex models with many interfaces and a large number of light rays. TracePro®, the commercially available ray tracing program employing the Monte Carlo method, was used in this project for more detail understanding of the experimental systems described in previous chapter. It was also used to compare the attenuation of optical fibers and ESR film tubes with different length and the state of the illumination switch in order to choose.

6.1.1 Model Set-Up on Monte Carlo Ray Tracing Program

Figure 6-1 shows the model set-up on TracePro® for simulating the change in intensity at the focal point of the Fresnel lens when the lens was activated and deactivated.

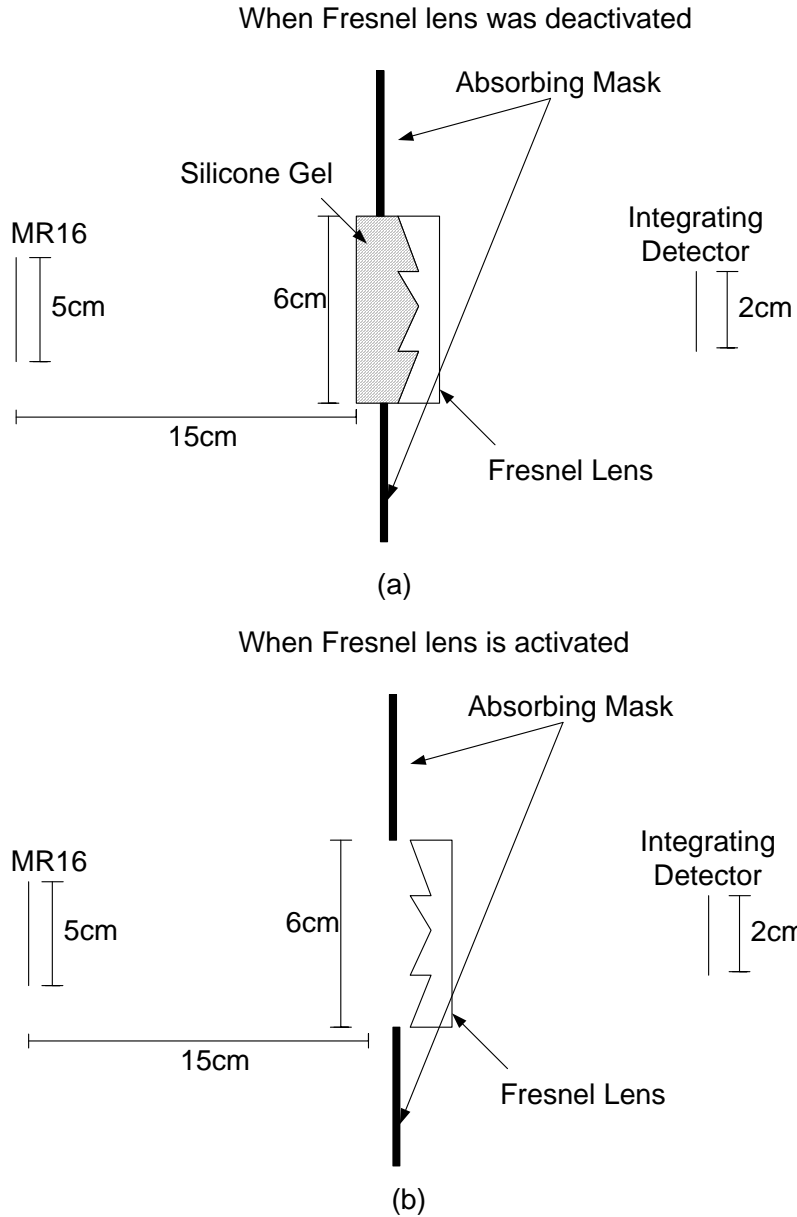


Figure 6-1. Set up for the ray tracing modeling (a) when Fresnel lens is deactivated and (b) activated (not to scale)

The simulated Fresnel lens had a focal length of 7.5 cm with a 6 cm diameter and refractive index of 1.49. Since the manufacturer of the Fresnel lens did not publish the exact geometry of the Fresnel lens, it was simulated by using the option that TracePro® had which created the Fresnel lens automatically by specifying the focal length of the lens, number of grooves, and its size. The difference between the simulated Fresnel lens and the actual Fresnel lens was the shape of the prisms. The simulated Fresnel lens had a prism that consisted of an

inclined slope (“surface B” in Figure 6-2 (a)) and a face parallel to the direction of the focus (“surface A”). On the other hand, the Fresnel lens used for the experiment had surface B with a slight angle on each prism as shown in Figure 6-2 (b). Since the geometry of the lens was not known exactly and matching the geometry of the actual Fresnel lens exactly with the simulated lens was not necessary for this preliminary simulation which was done only to check if the experimental results were not far off from simulation.

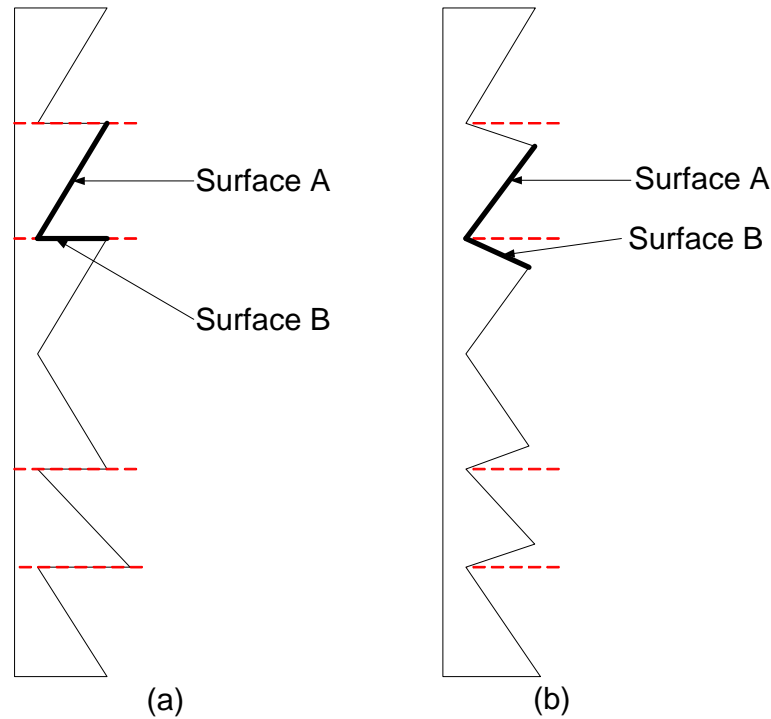


Figure 6-2. Schematic diagram of the (a) geometry of simulated Fresnel lens on TracePro and (b) the actual Fresnel lens for the illumination switch

There were a few different ways to simulate the light source on TracePro®. One way was to create a light source that had geometrically the same shape as the actual MR 16 with a small light bulb and mirror faces inside. However, there were too many mirror faces and the geometry of those was not published by the manufacturer so this method was hard to do. Another way of simulating the light source was to use the experimentally measured angular spectrum of the intensity of MR16 described in Chapter 5. TracePro® could simulate a light source by inputting relative angular intensity at all angles (0 to 90°). A table of inputted emissivity for simulating light source is shown in Table 6-1. Using these values, TracePro created light rays with intermediate angles by using a linear connection between the closest

angles. For example, the emissivity at 1.25° was 0.99 because the inputted emissivity at 0 and 2.5° was 1 and 0.98 respectively.

Table 6-1. Emissivity imputed for simulating the light source on TracePro

Angle	0	2.5	5	7.5	10	12.5	15	17.5	20	22.5	25
Emissivity	1	0.98	0.95	0.8	0.65	0.45	0.42	0.15	0.1	0.07	0.05

Figure 6-3 shows the angular dependence of the experimentally measured intensity level of the MR 16 and the simulated intensity level on the TracePro®. Although there was a small discrepancy, it was good enough for the feasibility study.

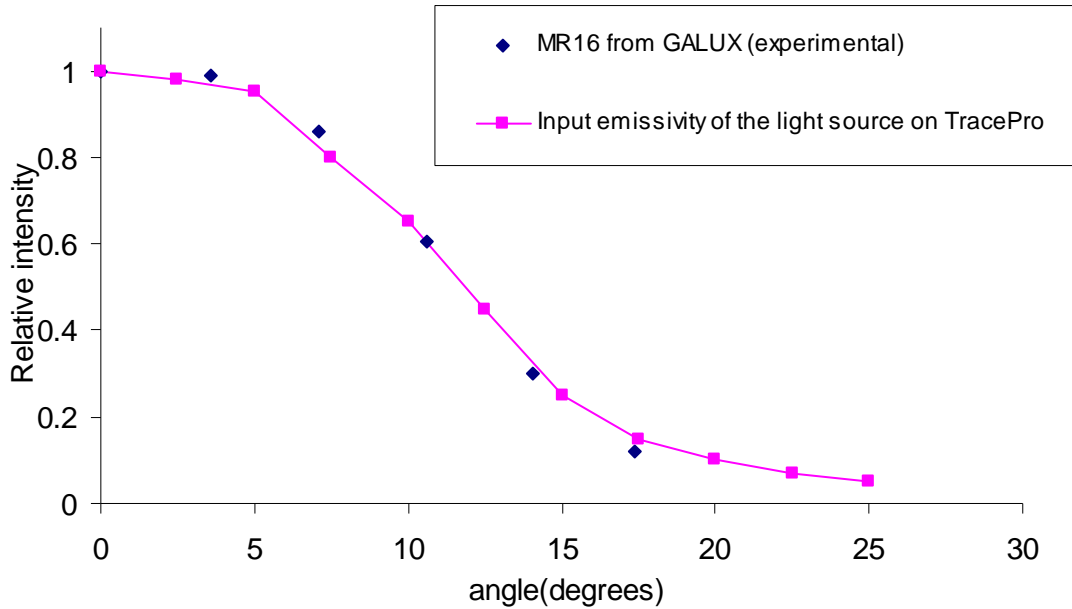


Figure 6-3. Graphs of experimentally measured intensity level of the MR16 and that of simulated light source

The simulated integrating detector was a detection plane with the same dimensions as the aperture of the integrating detector used in the experiment. The rays hitting the surface of this simulated integrating detector were counted in order to determine the intensity of the light entering the detector.

While the ray tracing was conducted using the simulated components described above, it was found that there were some rays that were not at the focal point of the Fresnel lens as shown in Figure 6-4 (which are called as misbehaved rays in this thesis). By checking the ray history of the simulated light rays, it was found that these misbehaved rays were caused by the surface B which sometimes did not properly redirect the incoming light to the focal point. When the incoming light was normal to the surface of the Fresnel lens, the number of misbehaved rays was about 5 % of the total number of incoming light at the Fresnel lens.

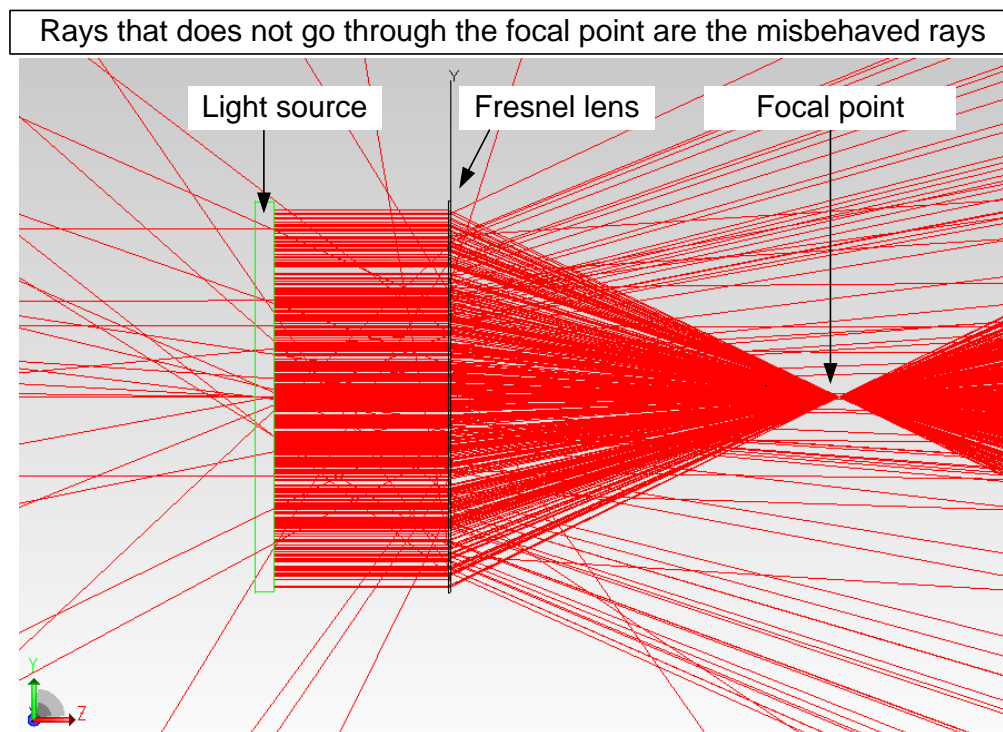


Figure 6-4. Simulated rays on TracePro (rays that does not go through the focal point are the misbehaved rays)

6.1.2 Model Results on Change in Intensity

Using the simulated set-up on TracePro described in the previous section, the change in intensity of the light at the focal point of the Fresnel lens was calculated. This was done by first counting the number of rays hitting the surface of the modeled integrating detector when the illumination switch was activated and deactivated. Then these values were used to calculate the simulated change in intensity of the light by using:

$$\text{Change in intensity(\%)} = 100 - \left(\frac{\# \text{ of rays when the device is deactivated}}{\# \text{ of rays when the device is activated}} \times 100 \right) \quad (6.1)$$

which was essentially the same quantity as was calculated in (5.2) where the change in intensity at the focal point was calculated based on the experimentally measured intensity. Figure 6-5 shows images from TracePro® for the cases where the Fresnel lens was activated and deactivated using a lens with a 7.5 cm focal length. It could be seen that the illumination switch was not focusing the light at the integrating detector when the Fresnel lens was deactivated (Figure 6-5 (a)). When the lens was activated, the light was focusing the light as shown on Figure 6-5 (b).

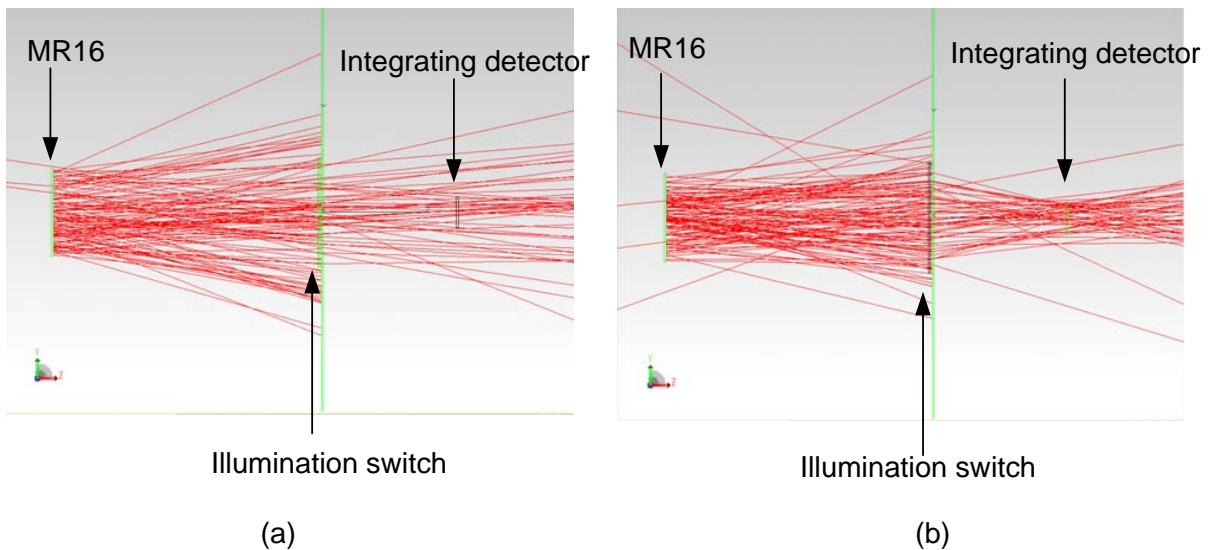


Figure 6-5. Images from TracePro when the device is (a) deactivated and (b) activated

The simulated change in intensity at the focal point was 81 % for the Fresnel lens with a 7.5 cm focal length.

6.2 COMPARISON WITH THE EXPERIMENTAL RESULT

The illumination switch with a Fresnel lens of $f=7.5$ cm resulted in a change in intensity of 74 % experimentally. The difference between this and the 81 % change in intensity resulted from the TracePro® model came from the discrepancy between the actual geometry of the Fresnel lens from the simulated one and also the simulated and actual angular distribution of

intensity level of the light source as described before. Another reason for this discrepancy came from the deformation of the silicone gel. In the ray trace modeling, the deformation of the silicone gel was simulated to be a perfect match with the shape of the Fresnel lens, but in the actual illumination switch, the silicone gel did not deform perfectly as was discussed previously. The total area of the silicone gel that was not in contact with the Fresnel lens was estimated to be about 10 %. The combinations of these differences in simulation and experiments produced the slight disagreement in the change in intensity. It was concluded that the experimental results were reasonable compared to the results from the ray tracing program considering these differences since the difference was only 6 %.

6.3 MODELING THE ESR FILM TUBES AND OPTICAL FIBERS

When the illumination switch is installed for a collimated daylighting system, transmitting devices is needed for guiding the light throughout a building. Since ESR film tubes and optical fibers are the candidates for solar canopy illumination system, they were modeled on the TracePro® to compare the anticipated performance associated with the illumination switch. In this chapter, the detailed TracePro® modeling of the ESR film tubes and optical fibers and their results are presented.

6.3.1 Comparison of ESR Film Tube and Optical Fiber on TracePro

The set up of the simulated model for this comparison was slightly modified from the previous section as shown in Figure 6-6.

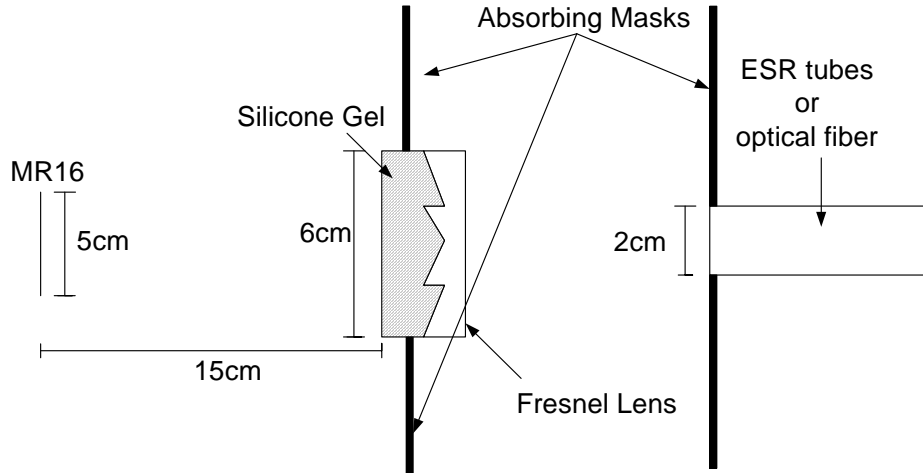


Figure 6-6. Set up of the ray tracing for comparing the optical fiber and ESR film tube

The simulated integrating detector was replaced first by an ESR film tube and then by an optical fiber. The simulated optical fiber had a cylindrical shaped rod with its index of refraction value of 1.49. The simulated ESR film tube was a hollow tube with a highly reflective property inside of the surface. Both the optical fiber and the ESR film tube had front surface of 2 cm in diameter. An absorbing mask was positioned around the aperture of the guide to absorb stray light rays. There were a few factors that were changed to compare the attenuation of the ESR film tube and optical fiber: the attenuation of the optical fiber per foot, the reflectance of the ESR film tube, their length, and the status of the illumination switch. The attenuation of the optical fiber was described by its attenuation per length. The attenuation of the ESR film tube was represented as reflectance of the multi-layered optical film. More loss in light intensity was caused by higher attenuation per length or smaller reflectance. The manufacturer of the optical fiber claimed that the attenuation was 1.5 % per foot⁷², but this quantity was measured previously to be about 4.5 % per foot⁷³. The reflectance of the ESR film was claimed to be about 98.5 %⁷⁴ and was measured previously to be between 98.5 % and 99.5 %⁷⁵.

Using TracePro®, the attenuation of the optical fiber could be controlled by specifying the absorption coefficient of the material which is calculated by:

$$\Phi_A = \Phi_0(1 - e^{-\alpha t}) \quad (6.2)$$

where Φ_A is the transmission loss in percentage per length, t is the length of the transmission loss in mm, and α is the absorption coefficient. For example, if the optical fiber has 1.5 % attenuation per foot, then $\Phi_A = 0.015$, $t = 1 \text{ foot} = 305 \text{ mm}$ which gives $\alpha = 4.95 \times 10^{-5}$.

Since both the ESR film tube and optical fiber had two different parameters that could be used to compare their attenuation, the best and worst cases of both transmitting devices were compared. In the best-case scenario, the attenuation of the optical fiber was 1.5 % per feet and the ESR film tube had 99.5 % reflectance. The comparison of different lengths of those light transmitting devices when the Fresnel lens was activated and deactivated is shown in Table 6-2.

Table 6-2. Transmittance loss for the best-case scenario

Length	10cm	50cm	150cm
ESR film tube (activated)	0.61 %	3 %	9.2 %
ESR film tube (deactivated)	0.28 %	1.47 %	4.2 %
Optical fiber (activated)	2.8 %	4.7 %	9.3 %
Optical fiber (deactivated)	2.9 %	4.8 %	9.3 %

In this table, “activated” means when the device was activated (i.e the light rays were focused at the focal point of the Fresnel lens) and “deactivated” means when the Fresnel lens was deactivated (i.e the light rays were not focused). The difference between the Fresnel lens being activated and deactivated was the divergence angle of the incoming light. When the Fresnel lens was activated, the incoming light for the transmitting device had a greater divergence angle than it did when the lens was deactivated.

The attenuation was calculated by using:

$$\text{Attenuation (\%)} = \frac{I_{\text{front}} - I_{\text{back}}}{I_{\text{front}}} \times 100 \quad (5.2)$$

where I_{front} is the intensity of the incoming light at the beginning of the transmitting device and I_{back} is the intensity of the outgoing light at the end of the transmitting device.

Table 6-2 shows that the difference between each state of the Fresnel lens for ESR film tube was much larger than that of the optical fiber. There was almost no difference for the optical fiber but the attenuation in ESR film tube when the Fresnel lens was activated was two to three times as much as when it was deactivated. With the length of 150 cm, the attenuation of the ESR film tube was only half of the attenuation of the optical fiber when the Fresnel lens was deactivated. On the other hand, the attenuation of ESR film tube and the optical fiber was very close when the Fresnel lens was activated. Recall that the activated state of the Fresnel lens had more divergent incoming light than deactivated state, meaning that there were more number of reflection that light rays experienced inside of the transmitting devices. This indicates that the ESR film tube have a small attenuation compared to the optical fiber when there is a small number of reflection but ESR film tubes are not suitable as light guiding device when the number of reflection is large.

The increase in attenuation as the length of the devices became longer was also larger for ESR film tubes. When the length of the ESR film tube was increased by a factor of five, the attenuation also increased by a factor of five. On the other hand, increasing the length of the optical fiber by five increased the attenuation only by a factor of two. This result also indicates that ESR film tubes increases its attenuation larger than the optical fibers when the number of reflection of the light rays increases.

For the worst-case scenario, the attenuation of the optical fiber was changed to 4.5 % per foot and reflectance of the ESR film tube was 98.5 %. The attenuation for this case is shown on Table 6-3.

Table 6-3. Transmittance loss for the worst-case scenario

Length	10 cm	50 cm	150 cm
ESR film tube (activated)	2.0 %	9.6 %	18.2 %
ESR film tube (deactivated)	0.95 %	4.1 %	11.4 %
Optical fiber (activated)	3.8 %	9.4 %	22.1 %
Optical fiber (deactivated)	3.3 %	9.4 %	21.9 %

As expected, the relative change in attenuation was similar to that of the best-case scenario, since the increase in attenuation was larger for ESR film tubes for longer length or more number of reflections.

In conclusion, the ESR film tubes have a very small attenuation compared to optical fibers when the length is short or the number of reflections is small. It was also concluded that if the length of the transmitting device is within 150 cm, then it is better to use the ESR film tube as a light guide since it has smaller attenuation at all times. The suitable material should be chosen for the light guides for collimated daylight collection systems depending on the necessary length and the collimation of the light in the light guides.

6.3.2 Advantages and Disadvantages of the ESR Film Tube and Optical Fiber

The previous section showed that if the length of the light guide is less than 150 cm, then ESR film tubes are more appropriate since the attenuation is smaller than that of optical fibers. However, there are other factors to consider in addition to attenuation. For example, the weight of the guide is important, since a heavier guide will require a more complex structural mounting system, and in many cases, a substantially heavier guide may be considerably more expensive. In comparison to optical fibers, ESR film tubes have the advantage of being hollow and therefore lightweight. In contrast, one disadvantage of the ESR film tubes is that it is harder to bend its shape when using them for a corner. Optical fibers are easier to bend because it is more flexible than ESR film tubes. Both ESR film tubes and optical fibers can be inefficient when experiencing a corner, so it is necessary to do ray tracing to check how much light is lost around a corner when it is necessary to do so. These advantages and disadvantages of the ESR film tubes and optical fibers must be considered when choosing the light guides.

7 DEMONSTRATION OF THE ILLUMINATION SWITCH IN A LIGHT GUIDANCE SYSTEM

In order to show how an illumination switch can be used in conjunction with a collimated daylight system to vary the illumination level of individual fixtures and to redirect unused sunlight to another fixture, a demonstration set up was constructed. In this chapter, the set up of the demonstration are presented.

7.1 SET UP OF THE DEMONSTRATION

A demonstration of the illumination switch was constructed to show how the switch could be used in a collimated daylight system to change the illumination level of a fixture and also how it was able to redirect the unused sunlight to another fixture. In this demonstration set-up, two diffuse white light bulbs were used to represent two separate lighting fixtures. These light bulbs were selected since they were convenient and readily-available diffusers, and were effective for a visual comparison of the relative illumination level. The set-up of the demonstration is shown in Figure 7-1. The collimated light source emitted light into a 1 m long internally-reflective pipe with a diameter of 6.5 cm which carried the light from the source to the illumination switch, in order to ensure that the light source encountered the lens. If this light guide pipe was not used, like in the experimental set up explained in Chapter 5, then more diverged light rays tend to reach outer area of the Fresnel lens of the illumination switch. The 1 m long light guide randomizes the divergence angle of incident light hitting at a certain area of the lens, meaning that the more diverging light rays could enter also from inner area of the Fresnel lens as well as outer area. This changed the change in intensity at the focal point of the lens from previous experiment described in Chapter 5. Therefore, a Fresnel lens with 20 cm focal length was inserted besides the front opening of the light guide to prevent the randomization so that the demonstration set-up was close to the results from the previous experiments where the performance of the illumination switch was measured.

Figure 7-1 (a) shows the set up of the demonstration when the illumination switch was active, focusing the light at the Fresnel lens' focal point. There was a small mirror (labeled as mirror 1 in Figure 7-1 (a)) at the focal point whose size was approximately the same as the

waist of the focused light, which was about 1.5 cm in diameter. This mirror redirected the light into a 30 cm-long light guide which carried the redirected light to a light bulb which was used as a diffuser. Behind mirror 1, there was another Fresnel lens with its focal length of 7.5 cm, which was identical to the lens used for the illumination switch. This Fresnel lens focused light that was not redirected by mirror 1, and the focused light was redirected by mirror 2 into another light guide and light bulb.

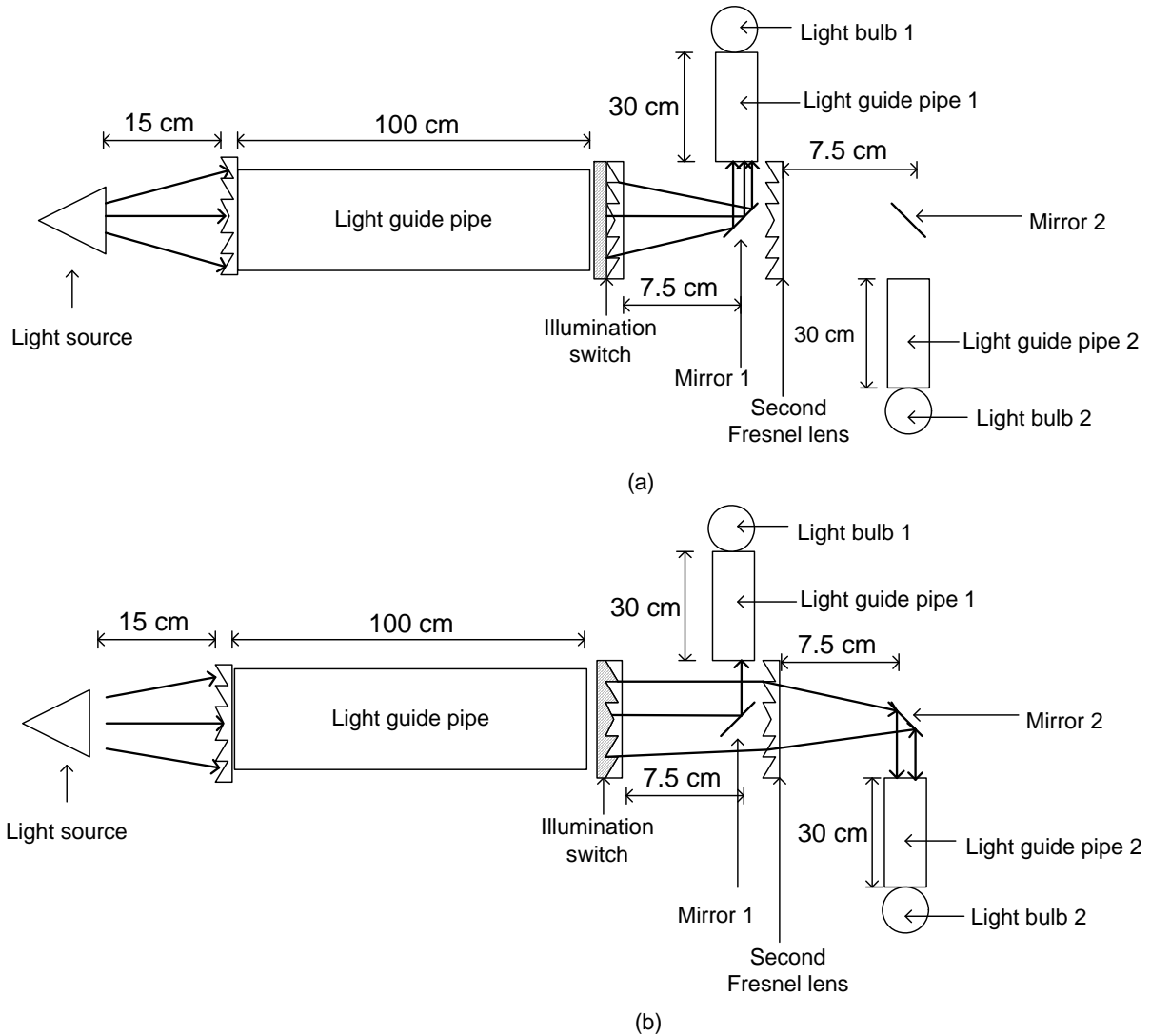


Figure 7-1. Schematic diagram of the demonstration when the lens was (a) activated and (b) deactivated

When the illumination switch was deactivated, a significant fraction of the light was no longer deflected by the first lens, as depicted by Figure 7-1 (b). Some of the light was

redirected by mirror 1 to the guide pipe 1 but most of the light was instead focused by the second Fresnel lens located behind the mirror 1. This light was redirected by mirror 2 and reached light bulb 2. In this state of the illumination switch, the intensity level of light bulb 1 was lowered from the previous state and the light bulb 2 became brighter. ESR film tubes were used as light guide pipes for this demonstration because the ray trace modeling showed that ESR film tubes have less attenuation than optical fibers for a length less than 150 cm as explained in Chapter 6. The ESR film tubes were mounted within a cylindrical tube so that the round cross-sectional shape was maintained along the length of the tube.

7.2 CONSTRUCTED DEMONSTRATION SYSTEM

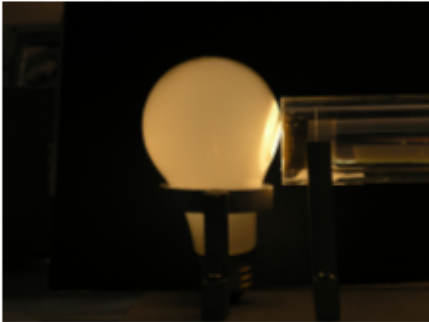
Some photographs of the constructed demonstration system are shown in Appendix E. The intensity levels diffused from light bulbs when the Fresnel lens was activated and deactivated was measured by a luminance meter⁷⁶ and their values are shown in Table 7-1.

Table 7-1. Illumination level of the light bulbs

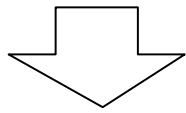
	Intensity of light bulb 1 (cd/m ²)	Intensity of light bulb 2 (cd/m ²)
Fresnel lens active	146 ± 1.5	31 ± 1.5
Fresnel lens deactivated	76 ± 1.5	121 ± 1.5

The change in intensity was 47.9 ± 1.1 % for light bulb 1 and 74.3 ± 3.7 % for light bulb 2. Since the light experienced the 1 m light guide before entering the illumination switch, the divergence of the incoming light was slightly different from the measurement set-up in Chapter 5 where there was no light guide pipe between the MR16 and the illumination switch. This accounted for the difference in intensity change from the measurements presented in Chapter 5. Although the change was slightly less than 50 %, the change in its intensity was visually obvious as shown on Figure 7-2. The intensity of light bulb 2 when the Fresnel lens was deactivated was lower than the intensity of light bulb 1 when the Fresnel lens was active. This was because some light hits mirror 1 and was redirected into light guide pipe 1.

Light bulb 2



Light bulb 1



Illumination switch turns on

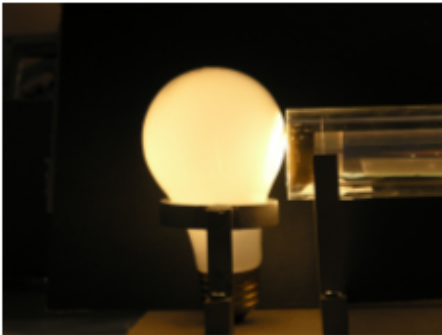
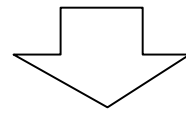


**Figure 7-2. Photographs of the light bulbs when the lens was activated and deactivated
(The light bulbs are used only for diffusing purpose)**

8 CONCLUSION

The goal of this project was to design and construct an illumination switch to be used in conjunction with a collimated daylight system in order to vary the illumination level of a fixture and to redirect the unused sunlight to another fixture for illumination.

The illumination switch for the solar canopy illumination system was constructed by using a converging Fresnel lens, a sheet of transparent silicone gel, and a pneumatic device to deform the silicone gel. The illumination switch originally focused incoming light at a focal point of the Fresnel lens and by locating a transmitting device at the focal point, it was possible to carry the light to each fixture and used it for illumination. This switch used a layer of soft, transparent silicone gel to control the focusing property of the Fresnel lens by deforming the gel into the structured surface of the Fresnel lens by pumping out the air between the silicone gel and the lens by a vacuum pump. Because of the hysteresis of the gel, in initial tests the gel did not separate from the Fresnel lens even after the pressure was released. In order to solve this problem, UV treatment on the surface of the silicone gel was used. UV treatment created a less sticky surface on the silicone gel which prevented the silicone gel from being stuck to the Fresnel lens. The vacuum pump was also used to help separate the silicone gel by applying negative pressure to the other side of the gel. With these adjustments to the device design, the illumination switch was successfully constructed and demonstrated.

There were a few factors which changed the performance of the illumination switch, such as the geometry of the Fresnel lens and the softness of the silicone gel. A Fresnel lens with shorter prisms, less number of grooves, and shorter focal length produced more change in intensity for the illumination switch. The silicone gel was UV treated for 30 minutes with the UV lamp. 30 minutes of UV treatment was concluded to be the optimum amount since the maximum change in intensity was the same as when there was no UV treatment and it also needed only about 10 kPa more pressure to reach the maximum change in intensity. Using a Fresnel lens from Edmund Optics which had a 7.5 cm focal length, the change in intensity was about 75 % when the light source with 38° beam angle was used as a light source. The divergence of the incoming light changed the performance of the switch. Considering that the divergence angle used was the worst case for the solar canopy

illumination system, the resulting change in intensity was a good result. This switch was also tested to check its endurance. The performance of the illumination switch was unchanged after 3000 switch cycles and also in a lower and a higher temperature environment (down to about 10 °C and up to about 60 °C).

The experimentally measured change in intensity of the illumination switch was compared with a simulated model using a ray trace program, TracePro®. The experimental result showed that the change in intensity was about 75 % and the simulated model showed that the change in intensity should be about 81 %. There were several differences between the experimental and the ray trace model. One of them was the slight difference in the geometry of the Fresnel lens and the shape of the silicone gel when it was deformed. Considering these differences, the experimental result was concluded to be within the error of the result of the ray trace modeling.

TracePro® was also used to compare the performance of the two different transmitting devices; ESR film tubes and optical fibers. The result showed that if the length of the transmitting device is shorter than 150 cm, then the ESR film tubes have slightly smaller attenuation whether the Fresnel lens is activated or deactivated. Considering the other advantages of the ESR films over optical fibers, such as the material cost and their lightweight, ESR film tubes were concluded more suitable for the solar canopy illumination system.

Lastly, the demonstration system was constructed for the illumination switch to show how it could be used in sunlight collection systems. The demonstration set up had a light source entering a 1 m long light guide and the illumination switch was located just after the light guide. It demonstrated that the light can be diverted from one fixture to another. This system switched the two light bulbs on and off depending on the status of the illumination switch. The illumination switch originally focused the light at one of the light bulbs. Once the Fresnel lens was deactivated and the illumination level of the first light bulb was lowered, the second light bulb became brighter.

The results of this project suggest that this pneumatic-based illumination switch can be used in collimated sunlight collection systems to vary the illumination level of a fixture. In

addition, it can be used to redirect the unnecessary sunlight from one fixture to the other. The constructed illumination switch successfully varied the intensity level enough to visually see the intensity change but this was only a preliminary experiment. The maximum change in intensity could be improved from the initial illumination switch by selecting a different combination of Fresnel lens and silicone gel. For example, softer silicone gel may improve its deformation into the Fresnel lens, resulting in larger change in intensity. The constructed illumination switch also showed that it has a potential for a long-term endurance so that it can be installed in a collimated sunlight collection system without frequent maintenance.

In summary, the results of this project has showed that the pneumatic-based illumination switch can help reduce the amount of electrical lighting needs with more efficient distribution of the sunlight when the amount of obtained sunlight is not enough for the demand.

REFERENCES

- ¹ Energy Information Administration : Official Energy Statistics from the U.S. Government, 2003 CBECS Detailed Tables, <http://www.eia.doe.gov/emeu/consumption/index.html> (accessed July 27, 2009)
- ² Roche, L., *et al.*, “Occupant reactions to daylight in offices”, *Lighting Res. Technol.*, Vol. 32 (3), 119-126, 2000
- ³ Beltran, L., *et al.*, “The Design and Evaluation of Three Advanced Daylighting Systems: Light Shelves, Light Pipes and Skylights”, *Solar '94 Conference Proceedings, American Solar Energy Society*, 25-30, 1994
- ⁴ Ibid 3
- ⁵ Courret, G., *et al.*, “Design and assessment of an anidolic light-duct”, *Energy and Buildings*, Vol. 28, 79-99, 1998
- ⁶ Piccolo, A., *et al.*, “Effect of Switchable Glazing on Discomfort Glare from Windows”, *Building and Environment*, Vol. 44, 1171-1180, 2009
- ⁷ Gardiner, D., *et al.*, “High-Efficiency Multistable Switchable Glazing Using Smectic A Liquid Crystals”, *Solar Energy Materials & Solar Cells*, Vol. 93, 301-306, 2009
- ⁸ Eames, P., “Vacuum Glazing: Current Performance and Future Prospects”, *Vacuum*, Vol. 82, 717-722, 2008
- ⁹ Boyce, P., *et al.*, “Minimum Acceptable Transmittance of Glazing”, *Lighting research and Technology*, Vol.27(3), 145-152, 1995
- ¹⁰ Ibid 3
- ¹¹ Whitehead, L., *et al.*, “A Cost-Effective Approach to Core Daylighting”, 445-450, 2006
- ¹² Muhs, J., *et al.*, “Design and Analysis of Hybrid Solar Lighting and Full-Spectrum Solar Energy Systems”, *SOLAR 2000 Conference Proceedings, American Solar Energy Society*, 16-21, 2000
- ¹³ SolarPoint™ Lighting, manufactured by Sunlight Direct. Inc., CA, 92128, USA
- ¹⁴ Parans Solar Lighting, manufactured by Parans, Gothenburg, Sweden
- ¹⁵ Parans Solar Lighting, Product outline, <http://www.parans.com/ParansProducts/ParansDownloads/tabid/903/Default.aspx> (accessed on July 27, 2009)

- ¹⁶ Rosemann, A., *et al.*, “Development of a Cost-effective Solar Illumination System to Bring Natural Light Into the Building Core”, *Solar Energy*, Vol. 40, 77-88, 2008
- ¹⁷ Ibid 16
- ¹⁸ Ibid 16
- ¹⁹ Ibid 2
- ²⁰ Bruce, V., *et al.*, *Visual Perception, physiology, psychology, and ecology*, 4th ed., Psychology Press, 2004
- ²¹ Whitehead, L., *et al.*, “A Cost-Effective Approach to Core Daylighting”, 445-450, 2006
- ²² Vikuiti Enhanced Specular Reflector Films, manufactured by 3M Company, St. Paul, MN, 55144-1000, USA
- ²³ Hecht, E., *Optics*, 4th ed., p197-200, Addison Wesley, United States, 2002
- ²⁴ Callow, J., *et al.*, “Air-clad optical rod daylighting system”, *Lighting Res. Technol.*, Vol. 35, 31-38, 2003
- ²⁵ Liang, D., *et al.*, “Fiber-Optic Solar Energy Transmission and Concentration”, *Solar Energy Materials and Solar Cells*, Vol.54, 323-331, 1998
- ²⁶ Kribus, A., *et al.*, “Optical Fibers and Solar Power Generation”, *Solar Energy*, Vol. 68 (5), 405-416, 2000
- ²⁷ Weik, M., *et al.*, *Fiber Optics Standard Dictionary*, 3rd ed, p4, Chapman and Hall, 1997
- ²⁸ STA-FLEX “SEL” End Light Optical Fiber, manufactured by Lumenyte International Corporation, CA, 92610, USA
- ²⁹ Ibid 22
- ³⁰ Leutz, R., *et al.*, *Nonimaging Fresnel Lenses: Design and Performance of Solar Concentrators*, p53, Springer, 2001
- ³¹ Vogel, R., US Patent # 3 409 347, November 5, 1968
- ³² Creff, R., US Patent #4 794 504, December 27, 1988
- ³³ Tripanagnostopoulos, Y., *et al.*, “The Fresnel Lens Concept for Solar Control of Buildings”, *Solar Energy*, Vol. 81, 661-675, 2007
- ³⁴ O’Neill, Mark., *et al.*, US Patent # 6 075 200, June 13, 2000

- ³⁵ Leutz, R., *et al.*, “Design of a Nonimaging Fresnel Lens for Solar Concentrators”, *Solar Energy*, Vol. 65 (6), 379-387, 1999
- ³⁶ Ibid 23, p474
- ³⁷ Paschotta, R., *Encyclopedia of Laser Physics*, p225-226, Wiley-VHC, 2008
- ³⁸ Fresnel lens, Product Identification Number CF40-0.5, manufactured by Nihon Tokushu Kogaku Jushi Co., Ltd, Tokyo, 175-0081, Japan
- ³⁹ Fresnel lens, Product Identification Number NT32-682, manufactured by Edmund optics Inc, NJ, 08007-1380, USA
- ⁴⁰ Fresnel lens, Product Identification Number NT32-590, manufactured by Edmund optics Inc, NJ, 08007-1380, USA
- ⁴¹ Dow Corning,
http://www.dowcorning.com/content/about/aboutmedia/silicon_technology_index_page.asp (accessed on July 27, 2009)
- ⁴² Zhang, H., *et al.*, “The Permeability Characteristics of Silicone Rubber”, *Fall Technical Conference Proceedings, Society for the Advancement of Material and Process Engineering*, 2006
- ⁴³ Dow Corning, Silicon Technology,
<http://www.dowcorning.com/content/sitech/sitechms/> (accessed on July 27, 2009)
- ⁴⁴ Dow Corning, Silicon Technology,
http://www.dowcorning.com/content/about/aboutmedia/silicon_technology_index_page.asp (accessed on July 27, 2009)
- ⁴⁵ Dow Corning, Silicon Technology,
http://www.dowcorning.com/content/sitech/sitechbasics/siloxane_polymerization.asp
- ⁴⁶ Sylgard 527 A&B Silicon Dielectric Gel, manufactured by Dow Corning Corporation, MI, 48684-0994, USA
- ⁴⁷ DowCorning, <http://www.dowcorning.com/> (accessed on July 27, 2009)
- ⁴⁸ Missinne, J., *et al.*, “An Array Waveguide Sensor for Artificial Optical Skins”, *SPIE Proceedings*, Vol. 7221, 2009
- ⁴⁹ Coope, R., *et al.*, “Modulation of retroreflection by controlled frustration of total internal reflection”, *Applied Optics*, Vol. 41 (25), 5357-5361
- ⁵⁰ Efimenko, K., *et al.*, “Aurface Modification of Sylgard-184 Poly(Dimethyl Siloxane) Networks by Ultraviolet and Ultraviolet/Ozone Treatment”, *Journal of Colloid and Interface Science*, Vol. 254, 306-315, 2002

- ⁵¹ Olah, A., *et al.*, “Hydrophobic Recovery of UV/Ozone Treated Poly(Dimethylsiloxane): Adhesion Studies by Contact Mechanics and Mechanism of Surface Modification”, *Applied Surface Science*, Vol.239, 410-423, 2005
- ⁵² Ibid 40
- ⁵³ Duoseal Two Stage Vacuum Pump 1400, manufactured by Sargent-Welch, NY, 14217, USA
- ⁵⁴ DC Based Solid State Relay, Product Identification Number Z120D10, manufactured by Opto 22, CA, 92590-3614, USA
- ⁵⁵ Three-way Quick Exhaust Normally Closed Valve, Product Identification Number 04F35C1116ACF4C05, manufactured by Parker Hannifin Corporation, MS, 39110, USA
- ⁵⁶ Two-Way, Normally Closed Valve, Product Identification Number S211GF02K4CG1, manufactured by GC Valves, CA, 93063, USA
- ⁵⁷ SphereOptics, Integrating Sphere Design and Application, <http://www.sphereoptics.com/assets/sphere-optic-pdf/sphere-technical-guide.pdf> (accessed July 27, 2009)
- ⁵⁸ Ibid 57
- ⁵⁹ High-Sensitivity Light-to-Voltage Converter, Product Identification Number TSL 257, manufactured by Texas Advanced Optoelectronic Solutions Inc., TX, 75074, USA
- ⁶⁰ IR Cutoff Filter, Product Identification Number NT53-710, manufactured by Edmund optics Inc, NJ, 08007-1380, USA
- ⁶¹ LabView Data Acquisition System, manufactured by National Instruments Corporation, Texas, 78759-3504, USA
- ⁶² High Temperature Accuracy Integrated Silicone Pressure Sensor, Product Identification Number MPXV6115VC6U, manufactured by Freescale Semiconductor, Inc.,TX, 78735, USA
- ⁶³ UV Light Curing Flood Systems, Product Identification Number 5000-EC, manufactured by Dymax Corporation, CT, 06890, USA
- ⁶⁴ Mercury Replacement Bulb, Product Identification number 36970, manufactured by Dymax Corporation, CT, 06890, USA
- ⁶⁵ <http://www.defelsko.com/technotes/DollyPreparation.htm> (accessed on July 29, 2009)

- ⁶⁶ Logger Pro 3, manufactured by Vernier Software & Technology, OR, 97005-2886, USA
- ⁶⁷ Stokes, D., “Characterisation of Soft Condensed Matter and Delicate Materials Using Environmental Scanning Electron Microscopy”, *Advanced Engineering Materials*, Vol. 3 (3), 126-130, 2001
- ⁶⁸ Mikula, R., *et al.*, “Characterization of Emulsions and Suspensions in the Petroleum Industry Using Cryo-SEM and CLSM”, *Collids and Surfaces*, Vol. 174, 23-36, 2000
- ⁶⁹ Habold, C., *et al.*, “Observations of the Intestinal Mucosa Using Environmental Scanning Electron Microscopy (ESEM); Comparison with Conventional Scanning Electron Microscopy (CSEM)”, *Micron*, Vol. 34, 373-379, 2003
- ⁷⁰ Ibid 67
- ⁷¹ TracePro 5.0.1, manufactured by Lambda Research Corporation, MA, 01460, USA
- ⁷² STA-FLEX “SEL” End Light Optical Fiber, manufactured by Lumenyte International Corporation, CA, 92610, USA
- ⁷³ Payne, M., “Attenuation of 20 Feet of 0.5” Plastic Optical Fiber (March, 7, 2008)”, Laboratory Identification Number: 3100081, (SSP Lab Co-Op Laboratory Book, University of British Columbia, 2008),
- ⁷⁴ Vikuiti Enhanced Specular Reflector Films, manufactured by 3M Company, St. Paul, MN, 55144-1000, USA
- ⁷⁵ Mossman, M., Private Correspondence
- ⁷⁶ Luminance Meter, Product Identification Number BM-9, manufactured by Topcon Positioning Systems, Inc., CA, 94551, USA
- ⁷⁷ Spectral distribution of Mercury bulb from Dymax Corporation, obtained by e-mail on May 6th, 2008
- ⁷⁸ Dymax Corporation, UV curing flood system 5000-EC series, <http://www.dymax.com/> (accessed on July 29, 2009)
- ⁷⁹ Dow Corning, Sylgard 527 data sheet, [http:// www. dowcorning.com/](http://www.dowcorning.com/) (accessed on July 29, 2009)
- ⁸⁰ Edmund Optics, Fresnel lens technical data sheet, <http://www.edmundoptics.com/> (accessed on July 29, 2009)
- ⁸¹ Edmund Optics, Fresnel lens technical data sheet, <http://www.edmundoptics.com/> (accessed on July 29, 2009)

APPENDIX A: UV LAMP

A UV lamp from Dymax 63, product identification of 5000-EC UV Light Curing Flood System, was used for UV treatment on the silicone gel surface so that the surface became less sticky. A mercury bulb was used in this lamp and its spectral distribution is shown on Figure A- 1.

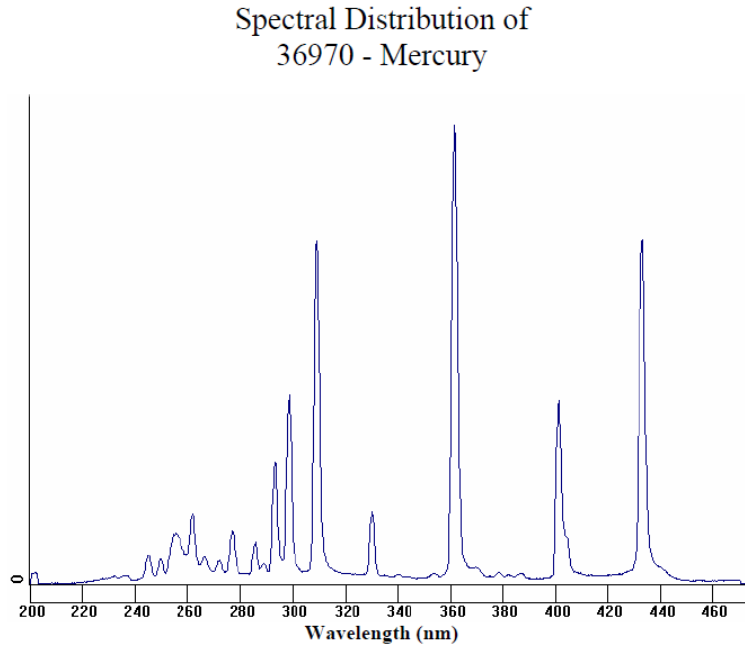


Figure A- 1. Spectral distribution of the mercury bulb used for the UV lamp⁷⁷

* The bulb degradation is < 20 % over 2,000 hours

Table A- 1. Some features of the UV lamp⁷⁸

Features	
Curing area	12.7 cm × 12.7 cm
Intensity	0.225 W/cm ²
Working distance	5 cm to 15 cm

APPENDIX B: SILICONE GEL

The silicone gel (Sylgard 527, silicone dielectric gel) from Dow Corning was used for the illumination switch. Its potential uses are mainly for sealing and protecting.

Table B- 1. Properties of the silicone gel from Dow Corning⁷⁹

Property	Value	Unit
Viscosity	0.425	Pas
Penetration	4.5×10^{-4}	m
Dielectric strength	15	Volts/m
Dielectric constant at 100 Hz	2.85	
Volume resistivity	7×10^{13}	Ohm-m
Operating temperature range	-45 to 150 °C / -49 to 302 °F	
Cure	Room temperature or heat cure	
Color	Clear	
Working time*	90 minutes	
Room temperature cure time	1 week	

*Working time is the time to double the viscosity.

APPENDIX C: FRESNEL LENS

The Fresnel lens from Edmund Optics, product number NT32-590, was used for the illumination switch.

Table C- 1. Properties of the Fresnel lens from Edmund Optics⁸⁰

Index of refraction	1.49
Transmission	92 % from 400-1100 nm
Maximum service temperature	80 °C

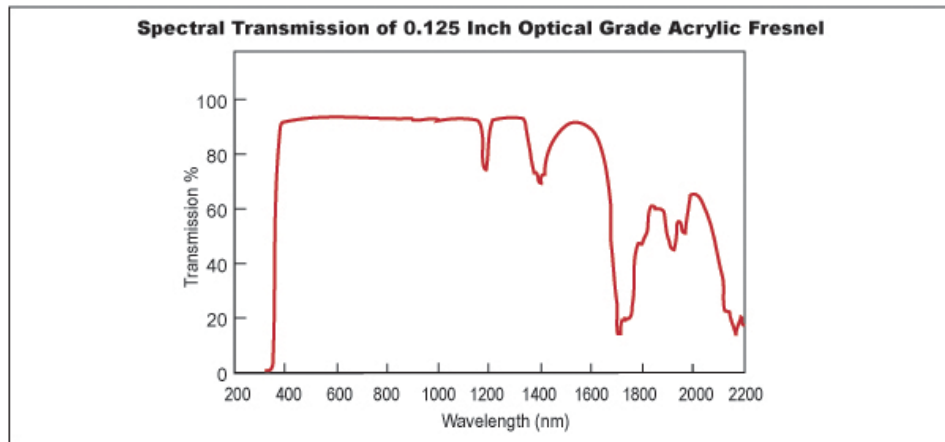


Figure C- 1. Spectral transmission of the Fresnel lens⁸¹

APPENDIX D: RAY TRACE MODELING

A ray trace modeling program, TracePro, was used in this project to compare its results with experimental results. Chapter 6 presented the set up and the results and more detail explanation of how it was modeled on TracePro are explained in this appendix. On TracePro, the silicone gel was simulated by first creating a cylindrical block with radius of 3 cm right besides the Fresnel lens. Then using a function called “subtract” on TracePro, a cylindrical block with one side of its surface negative replicated with the Fresnel lens could be created (Figure D- 1). This block was used when it was desired to simulate the Fresnel lens being deactivated by the silicone gel, meaning that the Fresnel lens was not able to focus the incoming light. This simulated silicone gel had a refractive index value of $n=1.4$.

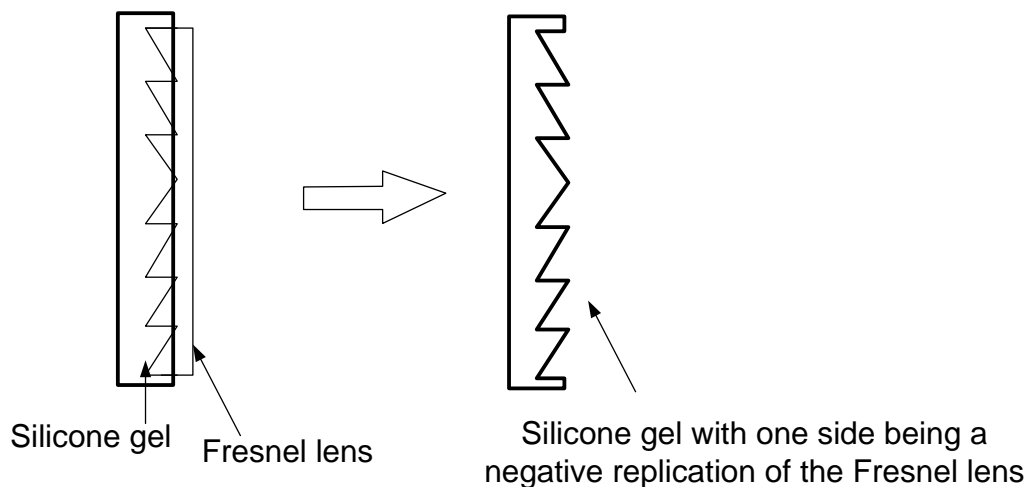


Figure D- 1. Simulated silicone gel by “subtraction”

On Figure 6-1, there was a tube with inner diameter of 6cm around the illumination switch. It perfectly absorbed light so any light that did not hit the illumination switch hit this tube to prevent any light outside of the illumination switch from entering the detector.

Polar Iso-Candela Plot was usually used as shown on Figure D- 2 when checking the angular distribution of incident angles on a surface. This figure shows the angular distribution when the light source entered a sheet of silicone gel, as an example.

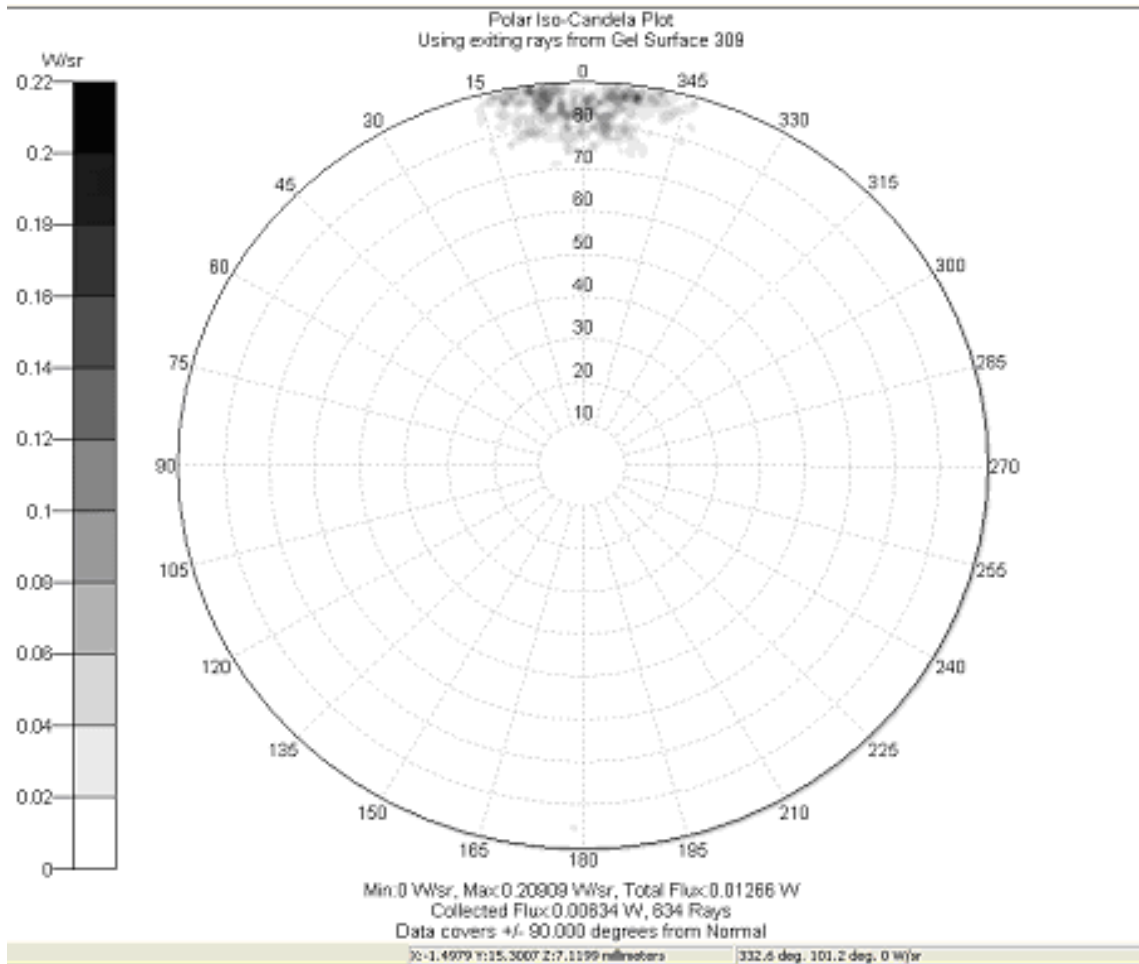


Figure D- 2. An example of Polar Iso-Candela Plot

APPENDIX E: PICTURES OF THE DEMONSTRATION SET UP

Chapter 7 presented the construction of the demonstration set up using the illumination switch. The picture of the demonstration set up is shown on Figure E- 1. The light source was hidden in the black box which prevented any light that did not go into the light guide from entering into the illumination switch. The light guide pipe propagated the light from MR16 to the illumination switch.

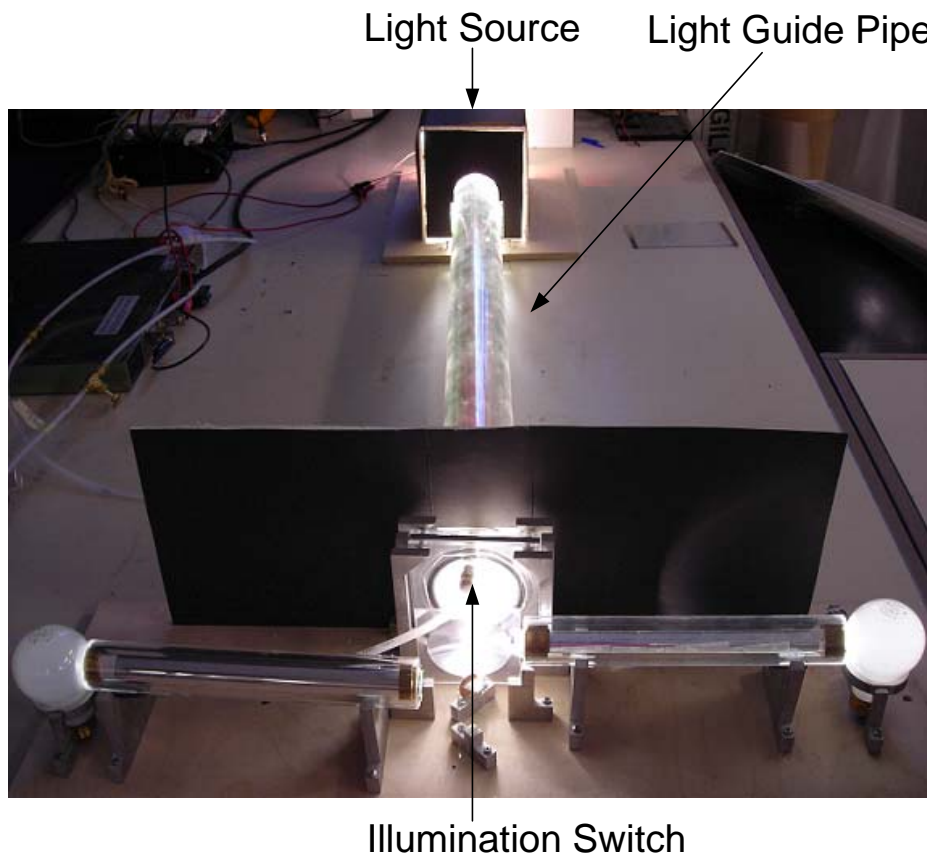


Figure E- 1. Picture of the demonstration set up

Closer look at the MR16 and the light guide pipe is shown on Figure E- 2. There was a Fresnel lens with focal length of 20 cm located just in front of the light guide pipe.

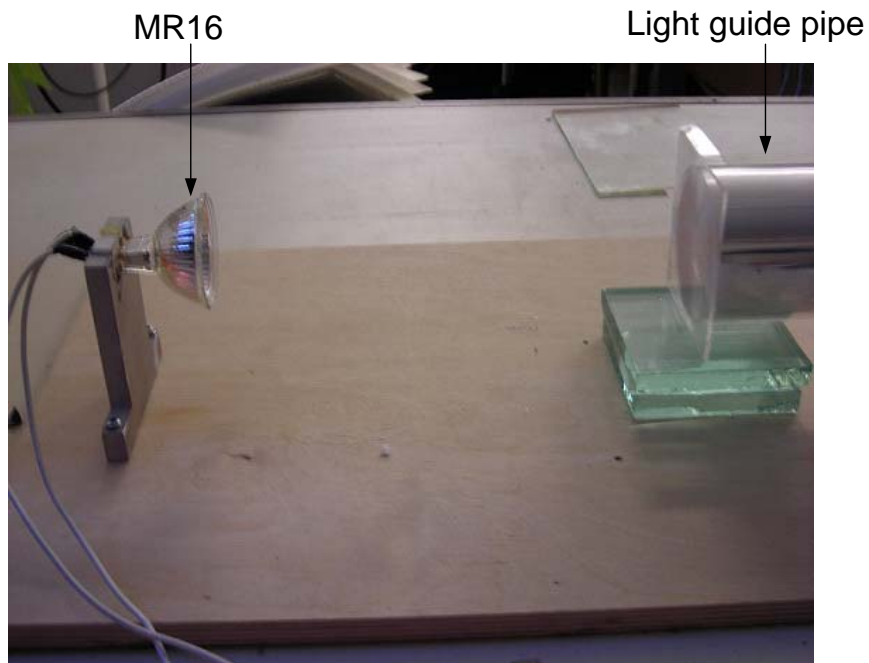


Figure E- 2. Closer look at the source light (MR16) and light guide

The closer look at the illumination switch, light guide pipes, mirrors, and light bulbs are shown on Figure E- 3. Each component was supported by stands which were bolted onto a wooden board so that it was well fixed. The ESR film tubes (light guide) were inserted in acrylic tubes since they could be easily ruined.

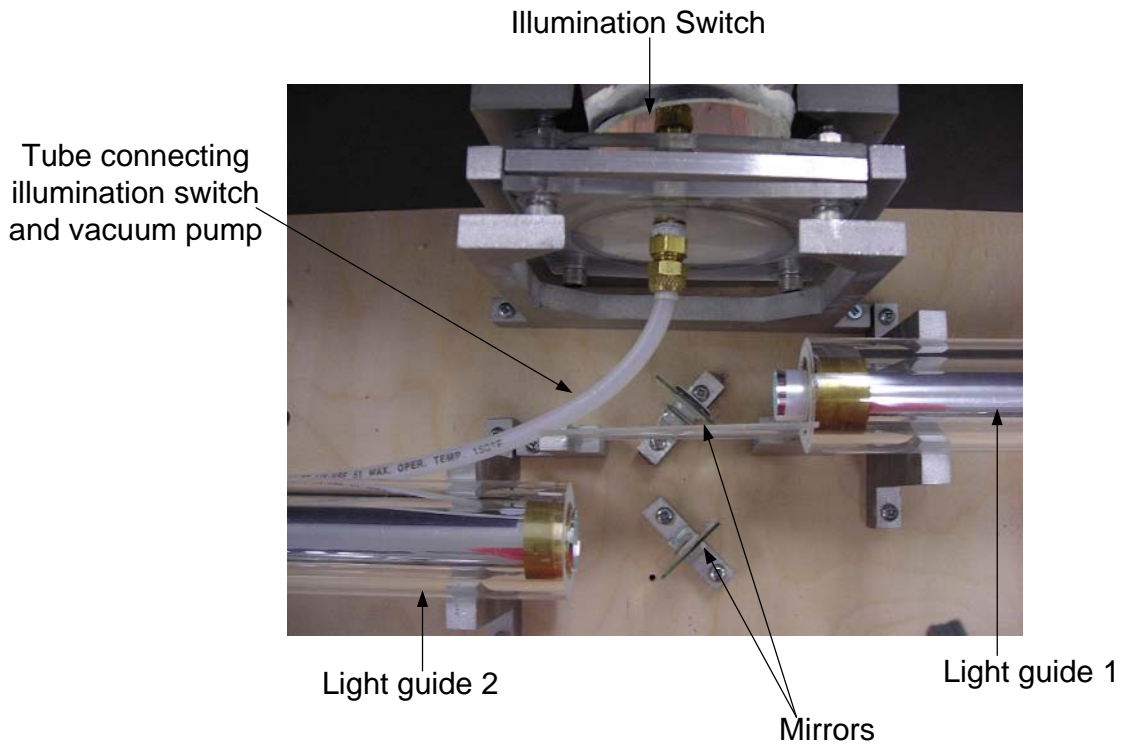
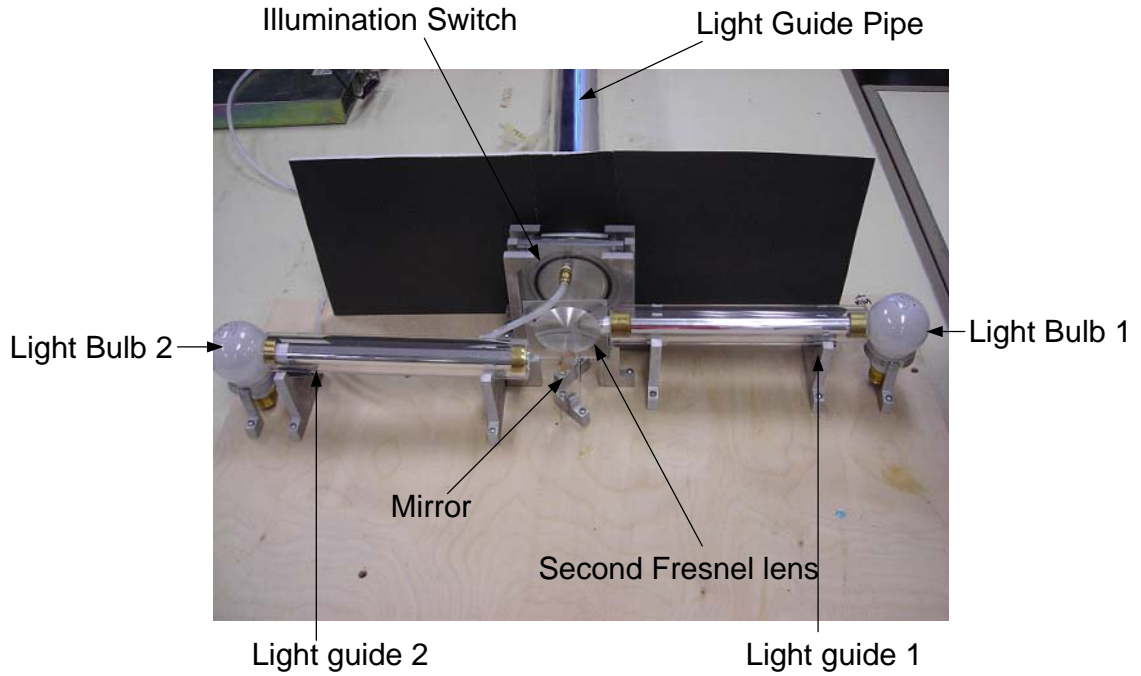


Figure E- 3. Closer look at the illumination switch and other optical components